Meteoritics & Planetary Science 42, Nr 7/8, 1441–1463 (2007)
Abstract available online at http://meteoritics.org

Trace element studies of silicate-rich inclusions in the Guin (UNGR) and Kodaikanal (IIE) iron meteorites

Gero KURAT[1*], Ernst ZINNER[2], and Maria Eugenia VARELA[3]

[1]Department of Lithospheric Sciences, University of Vienna, Althanstrasse 14, A-1090 Vienna, Austria
[2]Laboratory for Space Sciences and Physics Department, Washington University, Saint Louis, Missouri 63130, USA
[3]Complejo Astronómico El Leoncito (CASLEO), Av. España 1512 sur, J5402DSP, San Juan, Argentina
[*]Corresponding author. E-mail: gero.kurat@univie.ac.at

(Received 30 October 2006; revision accepted 20 June 2007)

Abstract–A devitrified glass inclusion from the Guin (UNGR) iron consists of cryptocrystalline feldspars, pyroxenes, and silica and is rich in SiO_2, Al_2O_3, and Na_2O. It contains a rutile grain and is in contact with a large Cl apatite. The latter is very rich in rare earth elements (REEs) (~80 × CI), which display a flat abundance pattern, except for Eu and Yb, which are underabundant. The devitrified glass is very poor in REEs (<0.1 × CI), except for Eu and Yb, which have positive abundance anomalies. Devitrified glass and Cl apatite are out of chemical equilibrium and their complementary REE patterns indicate a genesis via condensation under reducing conditions.

Inclusion 1 in the Kodaikanal (IIE) iron consists of glass only, whereas inclusion 2 consists of clinopyroxene, which is partly overgrown by low-Ca pyroxene, and apatite embedded in devitrified glass. All minerals are euhedral or have skeletal habits indicating crystallization from the liquid precursor of the glass. Pyroxenes and the apatite are rich in trace elements, indicating crystallization from a liquid that had 10–50 × CI abundances of REEs and refractory lithophile elements (RLEs). The co-existing glass is poor in REEs (~0.1–1 × CI) and, consequently, a liquid of such chemical composition cannot have crystallized the phenocrysts. Glasses have variable chemical compositions but are rich in SiO_2, Al_2O_3, Na_2O, and K_2O as well as in HFSEs, Be, B, and Rb. The REE abundance patterns are mostly flat, except for the glass-only inclusion, which has heavy rare earth elements (HREEs) > light rare earth elements (LREEs) and deficits in Eu and Yb—an ultrarefractory pattern.

The genetic models suggested so far cannot explain what is observed and, consequently, we offer a new model for silicate inclusion formation in IIE and related irons. Nebular processes and a relationship with E meteorites (Guin) or Ca-Al-rich inclusions (CAIs) (Kodaikanal) are indicated. A sequence of condensation (CaS, TiN or refractory pyroxene-rich liquids) and vapor-solid elemental exchange can be identified that took place beginning under reducing and ending at oxidizing conditions (phosphate, rutile formation, alkali and Fe^{2+} metasomatism, metasomatic loss of REEs from glasses).

INTRODUCTION

Iron meteorites are members of the large and highly heterogeneous class of differentiated meteorites and have bulk compositions far removed from that of the Sun. As such, they are widely believed to be the products of smelting processes, either on a planetary scale (planetary iron cores, "igneous irons") or on a planetesimal surface, small, impact-produced scale ("nonigneous irons"—for a recent summary, see Mittlefehldt et al. 1998). In either case, irons are believed to be the product of smelting, i.e., separation of metal from silicate in the liquid state with the help of gravity. Such a process—well known from industrial iron smelting—requires high temperatures as the liquid temperatures for both metal plus sulfide and chondritic silicate are well above 1300 K.

For decades, data have been accumulating that are incompatible with the steadfast belief that metal in iron meteorites crystallized from a metal melt (for a short recent summary, see Kurat 2003). One problem with a melt origin is that the most common matter in every planet, planetary mantle peridotites, is missing among meteorites. Another problem is posed by the presence of silicate inclusions and glasses in iron meteorites.

Silicate inclusions in iron meteorites (e.g., Bunch et al. 1970) display an astonishing chemical and mineralogical variety, ranging in their compositions from chondritic to highly fractionated, silica- and alkali-rich assemblages. Thus, they are believed to sample primitive (chondritic) as well as chemically fractionated parent bodies (e.g., Wasson 1985). Their origin(s) is commonly considered to be a simple one: the mixing of silicates, fractionated or unfractionated, with metal (e.g., Bunch et al. 1970; Wasson 1985; Scott 1979; Wasson and Wang 1986). The latter had to be liquid in order to accommodate the former in a pore-free assemblage, which all models accomplish by assuming shock-melting and shock-mixing. The process necessary to produce fractionated silicates in the first place is usually not addressed or impact shock events are suggested to be responsible.

IIE iron meteorites are particularly interesting because they contain an exotic zoo of silicate inclusions, some of which are chemically very strongly fractionated (e.g., Bunch et al. 1970; Prinz et al. 1983; Rubin et al. 1986; Ebihara et al. 1997; Ruzicka et al. 1999; Hsu 2003; Takeda et al. 2003). This extreme fractionation is commonly considered to be due to impact mixing and melting of feldspars and silica from the surface of a highly differentiated parent body (e.g., Ruzicka et al. 1999, 2006; Hsu 2003). But these meteorites pose a formidable conundrum (as do also other irons): young silicates are enclosed by very old metal (e.g., Burnett and Wasserburg 1967; Bogard et al. 1967; Harper and Jacobsen 1996; Birck and Allegre 1998; Bogard et al. 2000; Quitte et al. 2000, 2006; Snyder et al. 2001; Kleine et al. 2005; Schersten et al. 2006).

Thus, the origin(s) of silicate inclusions in iron meteorites was, and still is, a matter of debate. The following facts pose severe problems for the widely entertained model for the genesis of iron meteorites:

- metal is apparently older than inclusions (see references above)
- silicates are highly diverse in chemical composition
- silicates are distributed throughout the metal in spite of their much lower density
- silicates commonly form delicate aggregates that are fully preserved in the metal (see, e.g., Bunch et al. 1970; Nehru et al. 1982)

Besides their mineralogy and chemical composition, the main point to elucidate is the nature of the process that allows two different materials—high-density Fe-Ni metal and low-density silicate inclusions—to co-exist in a pore-free composite rock.

Here we report on chemical disequilibria in silicate-oxide inclusions in the Guin (UNGR) and Kodaikanal (IIE) irons. These inclusions are chemically extremely fractionated and indicate some relationship with enstatite meteorites and/or Ca-Al-rich inclusions (CAIs). Our studies show that the inclusions record nebular rather than planetary fractionation and metasomatic processes. Preliminary reports have been given by Kurat et al. (2005, 2006).

METHODS

We analyzed the nonmetallic phases in the Guin (UNGR) and Kodaikanal (IIE) irons for their major and minor element contents with a JEOL 6400 analytical scanning electron microscope (NHM, Vienna), a JEOL superprobe (Max-Planck-Institut für Chemie, Mainz, Germany) and a Cameca SX100 electron microprobe (Department of Lithospheric Sciences, University of Vienna, Vienna, Austria). Microprobe analyses were performed at 15 kV acceleration potential and 10 nA sample current. Mineral analyses were performed with a focused electron beam ~1 μm in diameter. Corrections were made by using the online ZAF program.

Trace element analyses of individual phases were made with the Cameca IMS 3f ion microprobe at Washington University, Saint Louis, USA, following a modified procedure of Zinner and Crozaz (1986a). Analyses were made with an O^- primary beam and energy filtering at low mass resolution was used to remove complex molecular interferences. The resulting mass spectrum is deconvolved in the mass ranges K-Ca-Sc-Ti, Rb-Sr-Y-Zr, and Ba-REE to remove simple molecular interferences that are not eliminated with energy filtering (Alexander 1994; Hsu 1995). Sensitivity factors for the REE are from Zinner and Crozaz (1986b) and those for other elements are from Hsu (1995). Absolute concentrations are calculated by normalizing the ion signals to that of Si, using the SiO_2 concentrations determined by electron microprobe analyses. Reported errors are 1 sigma and are due to counting statistics only.

RESULTS

Guin (UNGR)

Large silicate inclusions in Guin are common (Rubin et al. 1986) and consist of devitrified siliceous glass with or without augite, plagioclase, or phosphates. We investigated a part of an elongated oval devitrified glass inclusion (Fig. 1) taken from a slice (Guin A) that was cut from the main mass of Guin (Inv. Nr. M1141, NHM, Vienna). The inclusion appears macroscopically black and is enveloped by skeletal schreibersite. The boundary between the devitrified glass and schreibersite (as well as rust-sulfide objects) is very complex (Fig. 2a) with the phases tightly entangled, causing a very rough and very large surface of the former glass. The boundary is lined by a belt inside the former glass that is rich in small Fe oxide/sulfide inclusions. Cracks are abundant and mostly filled with rust. The devitrified glass does not contain phenocrysts but contains microlites (up to ~2 μm in length) and fine-grained (<10 μm) intergrowths of albite, silica, and low-Ca pyroxene with accessory clinopyroxene, ilmenite, rutile, FeNi metal, FeS, Cl apatite, and whitlockite. The rutile we investigated is located at the interface between the glass and the oxide/sulfide-rich object (Fig. 2b) and forms an elongated, apparently single crystal grain. The apatite we

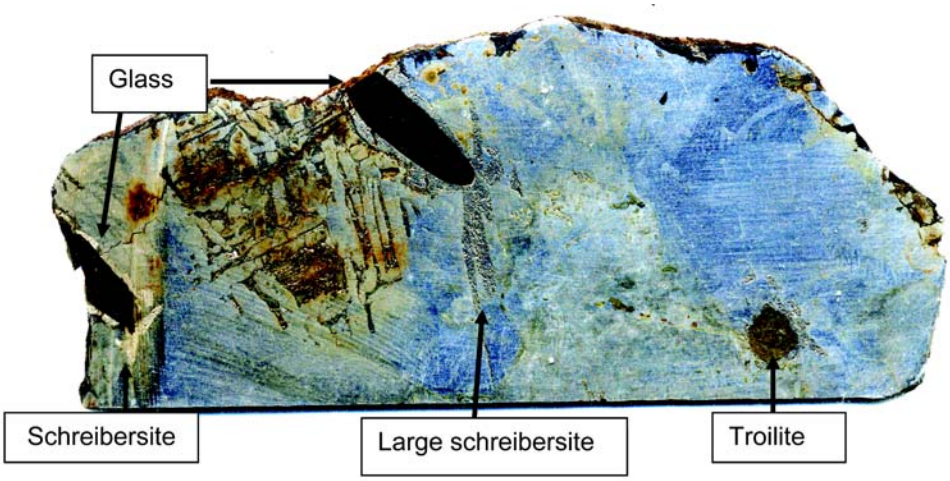

Fig. 1. Slice Guin A taken from the main mass of Guin at the Natural History Museum in Vienna (Inv. no. M 1141). Two glass inclusions (black) and one troilite (gray) are present. All inclusions are covered by schreibersite, which in addition is also present as a big plate cutting through the center of the slice ("large schreibersite"). The inclusion on the left edge was investigated in this study. Length of slice is ~9 cm.

investigated is also located at the interface between the former glass and schreibersite and is a large single crystal in contact with schreibersite. This contact is smoothly curved and in places decorated by rust (Fig. 2c). Magnetite forms euhedral crystals in inclusions consisting mainly of rust in the FeNi metal (Fig. 2d). Rust is omnipresent and is still forming at grain boundaries between schreibersite and metal and within schreibersite.

The phases of the devitrified glass are too small to be analyzed with the electron microprobe (EMP). Only apatite and rutile could be analyzed as individual minerals, otherwise we give the bulk composition of the former glass (Table 1). The latter is rich in silica, alumina, sodium, and potassium. The chemical composition is somewhat variable with ranges (in wt%) for SiO_2 66.0–72.2, TiO_2 0.15–1.0, Al_2O_3 15.8–19.6, FeO 0.69–4.2, CaO 1.17–1.47, Na_2O 7.8–10.3, and K_2O 0.59–1.0 (approximately chondritic Na/K). The former glass is very poor in Cr and Mn (below detection limit of the EMP), and has very little Mg (<0.02–0.04 wt% MgO) but some Cl (<0.02–0.10) and P_2O_5 (0.07–0.25). Rutile contains some SiO_2 (0.31 wt%), Cr_2O_3 (0.21), and FeO (0.48). The apatite contains Cl (6.0 wt%) and some SiO_2 (0.17), FeO (0.25), MnO (0.19), and Na_2O (0.39).

Trace element contents of the former glass are low (Table 2; Fig. 3). They are mostly at an abundance of ~0.1 × CI (CI = abundance relative to CI chondrites is defined as the mass ratio of the concentration in the sample and in CI chondrites), except for Zr, Ti, Nb, Sr, Ba, Be, K, and Rb (~10 × CI). Abundances of Sc, Ba, Yb, Li, and B are about chondritic. The rare earth element (REE) contents are also low (0.02–0.1 × CI) and decrease from La (~0.1 × CI) to Gd (~0.02 × CI) and increase again toward Lu (~0.1 × CI). Europium and Yb have positive abundance anomalies (at ~4 × CI and ~0.6 × CI, respectively) with respect of the other REEs. The chlorapatite co-existing with the devitrified glass has low Ti, V, Zr, Nb, Be, V, Cr, K, and Rb (<0.1 × CI), high Sr (~20 × CI), REE, and Y (~70–80 × CI) contents with a flat abundance pattern and negative anomalies in Eu and Yb (~43 × CI and ~16 × CI, respectively) abundances. Scandium, Ba, Mn, Li, and B have approximately chondritic abundances. Rutile is extremely poor in most trace elements, many of which were found to be below detection limits. Very low are the abundances of Y, REEs, Mn, and F (<0.1 × CI). The abundances of Sc, Sr, Ba, V, Cr, Li, and K are approximately chondritic and those of Zr (760 × CI) and Be (520 × CI) are extremely high. Magnetite is also very poor in trace elements, with most elements being below detection limits (REEs and high-field-strength elements [HFSEs]). Abundances below 0.01 × CI were found for Sc, V, Cr, and Li. Strontium, Ba, K, B, and F are present at ~0.1 × CI abundance levels.

Kodaikanal

The Kodaikanal sample investigated in this study was cut from the 4 mm thick large slice of the Natural History Museum in Vienna (Inv. no. H988) shown in Buchwald (1975). The sample was cut from the left lower corner. It contains three silicate inclusions that are embedded in FeNi metal (Fig. 4) and which we named inclusions 1, 2, and 3. All inclusions have mostly rounded and smooth surfaces and are in part covered by schreibersite as previously described (Bence and Burnett 1969).

Inclusion 1 consists exclusively of glass. It has the shape of a slightly deformed sphere with flat borders in three places. Schreibersite covers part of the inclusion as a very thin layer and a small amoeboid crystal (Fig. 4, detail). Inside the glass, a staircase of crystal faces leads down to a polygonal, flat bottom. Inclusions 2 and 3 are multiphase inclusions consisting of devitrified glass, augite, and low-Ca pyroxenes with chromite, apatite, and whitlockite as minor phases.

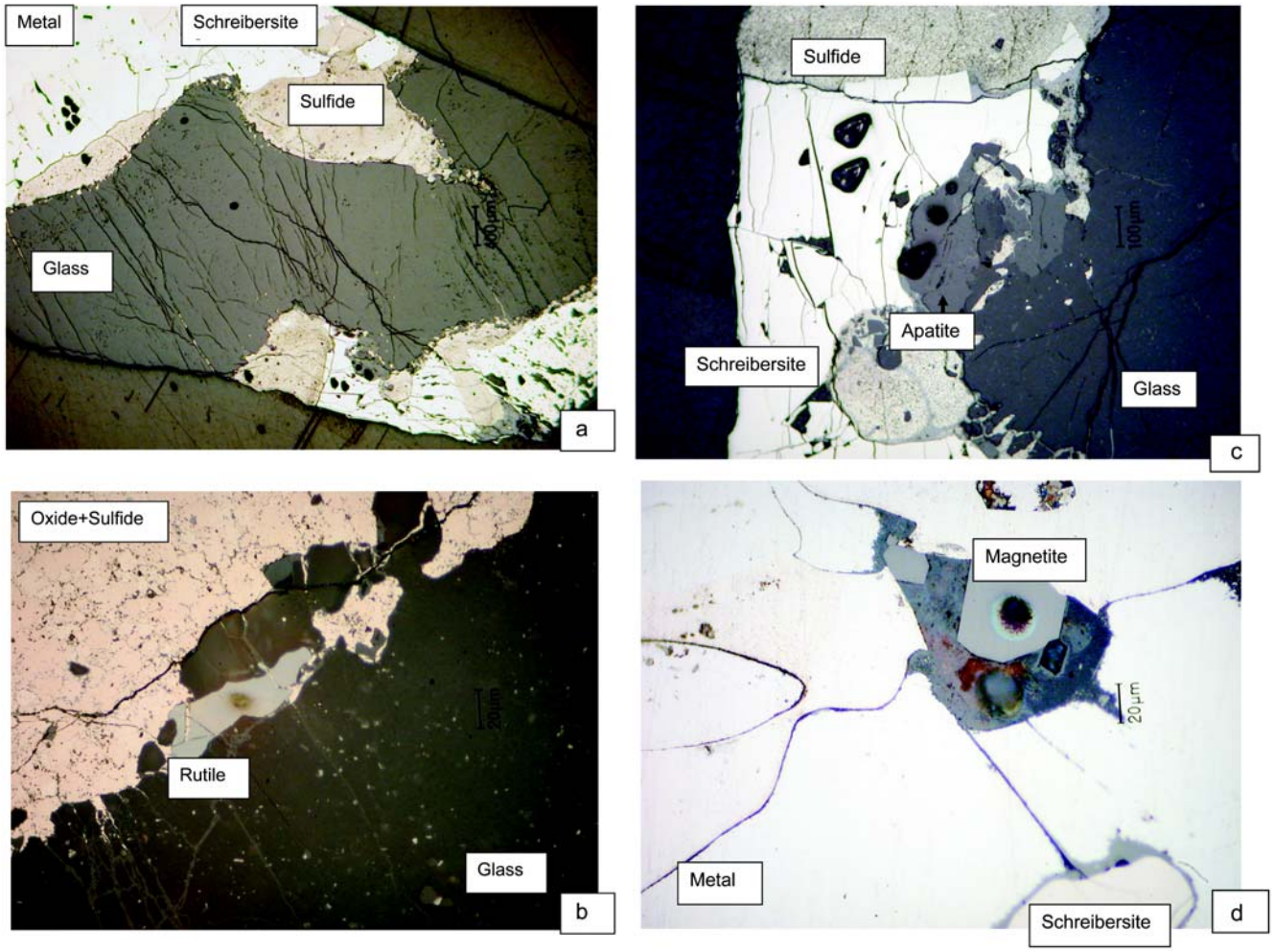

Fig. 2. a) Reflected-light image of section Guin A depicting devitrified glass (gray, rich in cracks) covered by sulfide plus rust (gray, lens-shaped objects upper center, center left and center bottom), schreibersite (white, covering the rust-sulfide objects on top and bottom), and metal (white, upper left corner). Black dots are ion probe sputtering pits. Scale bar is 400 μm. b) Close-up of the boundary between glass (dark), the lens-shaped sulfide/rust object from Fig. 2a (light gray, left upper corner) and rutile (gray). The complex boundary indicates incomplete separation of a (sulfide +/– X)-rich phase and the liquid. Note the cracks and the rutile in the center (with small ion probe sputtering pit) and the abundant microlites in the dark devitrified glass. Reflected light image. Scale bar is 20 μm. c) Large apatite crystal (center, gray) in contact with devitrified glass (dark gray, right side) and schreibersite (white, left side). Black areas in apatite and schreibersite are ion-probe sputtering pits. Reflected light image. Scale bar is 100 μm. d) Metal (white with rust-decorated lobate grain boundaries) with inclusions of rust (gray) enclosing euhedral magnetite (light gray) with central SIMS sputtering pit. Reflected light image. Scale bar is 20 μm.

Inclusion 2 (~9 mm in size) has pyroxenes—ranging in size from 500 μm to over 2000 μm—located in the center (Figs. 4 and 5). Anhedral to subhedral augites have bulky habits and commonly are overgrown by euhedral to subhedral skeletal crystals of low-Ca pyroxenes, which formed at the expense of the Ca-rich pyroxenes. Chromite is mainly associated with the pyroxenes and the pyroxene-glass interface. In many places, the clear glass with needle- and plate-like crystals of apatite and whitlockite dominate the near-surface volume of inclusion 2 (Fig. 6). The mineralogy of inclusion 3 and its phase composition are similar to those of inclusion 2, but the inclusion is located near a fracture (see Buchwald 1975, photo) and, consequently, it has some signs of alteration, as evidenced by the presence of areas with very thin Fe-rich threads, creating the impression of a net. Because of the alterations in this inclusion, we have decided to perform the trace element study in inclusions 1 and 2 only.

The major element chemical compositions of main phases in all inclusions are given in Table 3. Glasses in the three inclusions have similar chemical compositions and are all highly siliceous (SiO_2: 64.4–67.7 wt%), rich in TiO_2 (0.41–0.51), Al_2O_3 (17.8–19.4), Na_2O (4.1–7.1), and K_2O (2.7–6.4). They are poor in Cr_2O_3 (0.14–0.20 wt%), MnO (0.13–0.18), MgO (0.08–0.13), and CaO (0.10–0.21), but contain some FeO (0.48–1.19 wt%) and P_2O_5 (0.20–0.25). Clinopyroxenes are chemically homogeneous over large areas and are MgO-rich (17.0–18.0 wt%), Cr_2O_3-rich (~1.2) and poor in Al_2O_3 (~1.3) and Na_2O (0.50–0.73). Low-Ca

Table 1. EMP analyses of phases from Guin A (in wt%, N = number of analyses).

	Glass average	Glass Si-rich	Glass Na-rich	Glass K-rich	Glass Fe-rich	Rutile	Apatite
N	40	8	9	5	11	3	8
SiO_2	68.0	72.2	66.3	66.8	66.0	0.31	0.17
TiO_2	0.29	0.15	0.28	1.00	0.22	97.2	
Al_2O_3	17.8	15.8	19.6	17.8	17.2	0.03	
Cr_2O_3						0.21	
FeO	1.80	1.60	0.69	2.11	4.2	0.48	0.25
MnO							0.19
MgO	0.03	0.04		0.03	0.04	0.02	
CaO	1.31	1.17	1.47	1.30	1.22		52.8
Na_2O	9.0	7.8	10.3	8.8	8.4		0.39
K_2O	0.72	0.59	0.73	1.00	0.65	0.02	
P_2O_5	0.19	0.20	0.07	0.25	0.21	0.02	39.1
Cl	0.04	0.04		0.07	0.10		6.0
Total[a]	99.18	99.59	99.44	99.16	98.24	98.29	98.90

[a]Not corrected for O equivalent of Cl.

Table 2. Ion probe analyses of phases from Guin A (in ppm). Upper limits are marked in italics.

Element	Glass 1	Error	Glass 2	Error	Apatite	Error	Rutile	Error	Magnetite	Error
Li	1.95	0.03	2.73	0.03	3.1	0.05	0.8	0.1	0.011	0.005
Be	0.35	0.01	0.65	0.02	0.0036	0.0006	12.9	0.9	*0.004*	
B	1.06	0.04	1.98	0.05	1.3	0.05	1.1	0.2	0.08	0.03
F	0.15	0.01	0.13	0.01	4990	26	0.1	0.03	3.5	0.8
K	5771	4	5902	3	18.3	0.3	452	6	30	2
Ca	8869	3	8976	2.5			1914	44	49	8
Sc	4.5	0.1	4.2	0.1	2.78	0.05	12.5	0.5	0.016	0.007
Ti	3475	2	2420	1.5	7.5	0.4			*0.39*	
V	6.5	0.1	5.35	0.08	1.18	0.05	105	2	0.05	0.02
Cr	73	1.3	90	1	5.9	0.4	1056	21	0.77	0.35
Mn	223.6	0.7	378.5	0.8	1817	3	45	2	247	6
Fe	4137	3	5275	12	831	8	7830	92		
Rb	14.6	0.3	15.3	0.3	0.14	0.01	0.5	0.08		
Sr	59.9	0.4	61.1	0.3	154.8	0.7	4.6	0.6	0.5	0.1
Y	0.078	0.006	0.085	0.008	109	0.5	0.17	0.03		
Zr	30.6	0.9	45	1	0.41	0.05	3000	60	*0.32*	
Nb	4.5	0.15	3.8	0.1	0.006	0.001				
Ba	2.8	0.3	21.2	0.3	1.2	0.1	1.7	0.3	0.7	0.2
La	0.022	0.003	0.017	0.002	16.5	0.3	1	0.2		
Ce	0.03	0.003	0.036	0.002	38.3	0.45	1.3	0.2		
Pr	0.0045	0.001	0.0064	0.0008	4.8	0.1	3.6	0.5		
Nd	0.011	0.002	0.02	0.002	24.1	0.4	0.21	0.06		
Sm	0.007	0.003	0.012	0.003	6.3	0.3				
Eu	0.25	0.03	0.21	0.02	0.91	0.05	*0.04*			
Gd	0.004	0.002	0.0035	0.0017	10.2	0.4	*0.06*			
Tb	*0.0013*		0.0014	0.0005	1.9	0.1	*0.02*			
Dy	0.017	0.002	0.015	0.002	13.4	0.3	*0.04*			
Ho	0.007	0.001	0.008	0.001	3.2	0.1				
Er	0.017	0.003	0.016	0.002	9.01	0.25				
Tm			*0.004*		1.26	0.08				
Yb	0.132	0.008	0.087	0.005	2.5	0.2				
Lu	0.002	0.001	0.0036	0.0008	1.3	0.1				

pyroxenes are also mostly chemically homogeneous, with low CaO (~1.3 wt%) and Al_2O_3 (0.37) contents, but are fairly rich in TiO_2 (0.22), Cr_2O_3 (0.45), MnO (0.51), and FeO (10.4). Very thin, Fe-rich discontinuous rims have similar compositions, except for the FeO content, which is about 15 wt% and probably due to rust at the grain boundary. Chromite commonly associated with low-Ca pyroxene is rich in TiO_2 (3.4 wt%) and Cr_2O_3 (50.2) and contains appreciable amounts of Al_2O_3 (9.8), MnO (0.66), and MgO (6.0). Some SiO_2 (1.0 wt%) and ZnO (0.06) are also present. Apatite

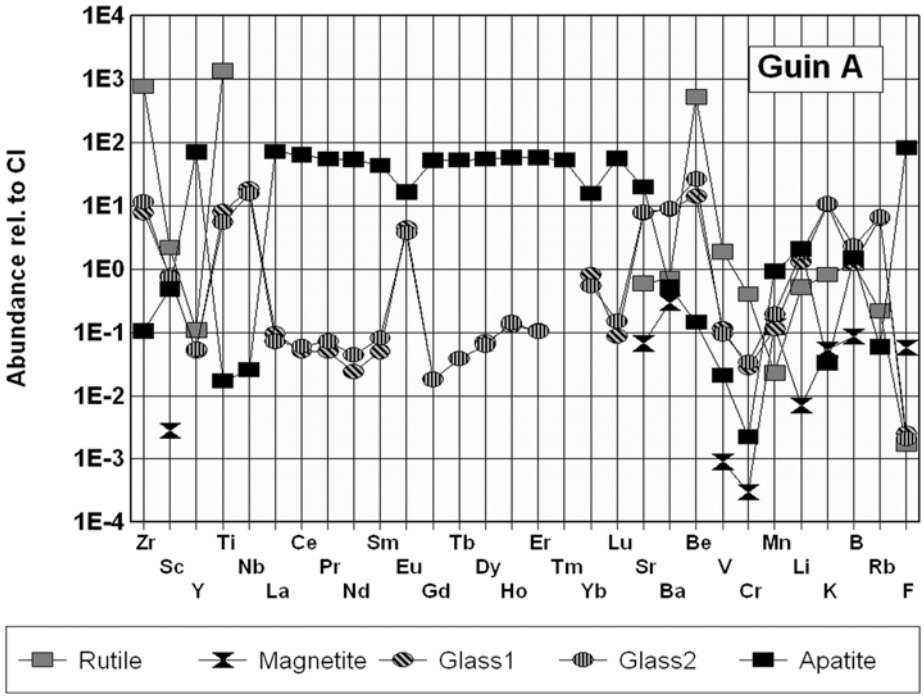

Fig. 3. CI-normalized trace element abundances in phases of the Guin A silicate-oxide inclusion (normalizing data from Anders and Grevesse 1989). Here and in the following graphs the elements are ordered according to decreasing condensation temperature (Lodders 2003), except for the REEs, which are ordered by increasing atomic number.

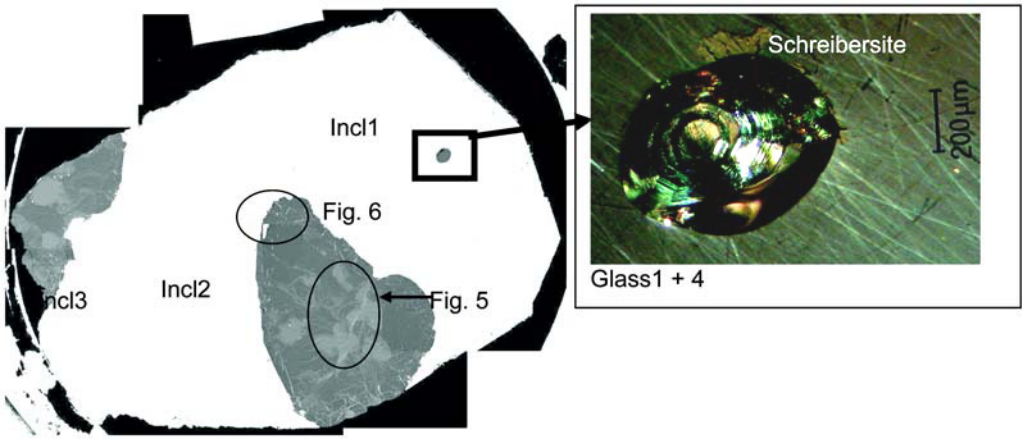

Fig. 4. Composite backscattered scanning (BSE) electron image of the polished section of Kodaikanal (from Inv. no. H988, NHM Vienna) investigated. Metal (white) contains 3 silicate inclusions (labelled Incl. 1, Incl. 2, and Incl. 3). Inclusion 1 is shown in an enlarged image at right, details of inclusion 2 in Figs. 5 and 6. Inclusion 1 is a pure glass inclusion; inclusions 2 and 3 are multiphase inclusions with a high proportion of devitrified glass. Note the clear glass of inclusion 1 that allows visibility to the bottom and the walls, which are decorated by steps of crystal faces. The total sample is 2.54 cm in diameter.

contains little SiO_2 (0.71 wt%), FeO (0.45), MgO (0.18), Na_2O (0.06), or Cl (0.25 wt%).

Trace element abundances as determined by ion microprobe analysis are presented in Table 4. Glasses of three different compositions have been encountered (Fig. 7). All glasses are poor in trace elements, except for Zr (~10 × CI), Nb (~15–200 × CI), Be (~45–120 × CI), B (~12–14 × CI), and Rb (200–400 × CI). The average trace element abundance pattern of the glasses is low in Sc, Y, REEs, Li, and F (~0.1–4 × CI) and very low in V, Cr, and Mn (<0.1 × CI). In the glass-only inclusion 1 (analyses Glass 1 and Glass 4) the heavy REEs (HREEs) are enriched (Lu ~ 3.7 × CI) over the light REEs (LREEs) (Ce ~ 0.43 × CI), with small negative anomalies in Eu and Yb abundances. This glass is the richest in Nb (~205 × CI), Be, B (~110 × CI), and Rb (~500 × CI) and the poorest in Eu (<0.26 × CI) and F

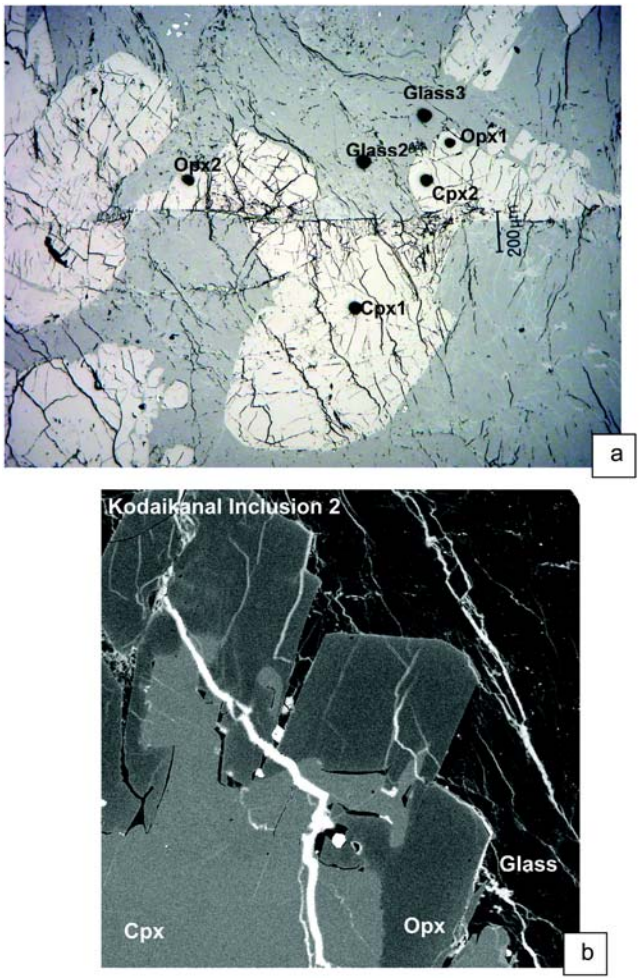

Fig. 5. a) Reflected light optical micrograph of clinopyroxene (Cpx, light gray), in part overgrown by low-Ca pyroxene (Opx), in the center of Kodaikanal glass-rich inclusion 2. The black ion probe sputtering pits are labelled in accordance with Table 4. Bright dots are small chromites inside pyroxenes and at the interface to the devitrified glass (gray). Scale bar is 200 µm. b) Backscattered electron (BSE) image of detail from inclusion 2 depicting clinopyroxene (Cpx, light gray) overgrown by low-Ca pyroxene (Opx, gray) and embedded in devitrified glass (dark, rich in cracks). Low-Ca pyroxene has crystal faces in contact with the glass and obviously grew from the former liquid by reaction between the liquid and the clinopyroxene. Small bright crystals in pyroxene and in glass are chromite. Side-length of picture is ~600 µm.

(~0.035 × CI). The second type of glass is represented by analyses Glass 2 and Glass 3. It is in contact with pyroxenes in the center of inclusion 2. In contrast to glass in inclusion 1, this glass has a flat REE pattern with approximately chondritic abundances and a small positive Eu anomaly and has less Nb (~20 × CI), Be (~50 × CI), and Cr (~0.0025 × CI). The third type is represented by Glass 5, which co-exists with abundant small apatites near the surface of inclusion 2 (Fig. 6). It has the lowest abundance of the REEs (0.13–0.45 × CI), except for Eu, which shows a large positive abundance anomaly (1.4 × CI). The REE abundances show a V-type

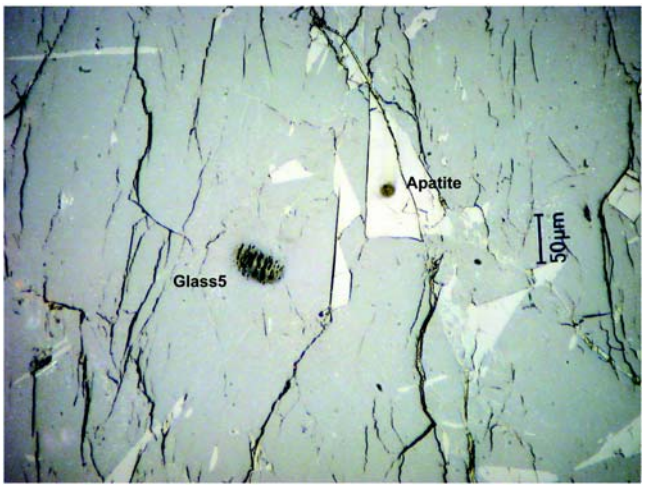

Fig. 6. Reflected light optical micrograph of part of Kodaikanal inclusion 2 (upper end in Fig. 4) depicting platy and skeletal apatite (light gray, approximately 10 vol%) in devitrified glass (gray). Ion probe sputtering pits in glass (Glass 5) and apatite are labelled in accordance with Table 4. Scale bar is 100 µm.

pattern with high La and Lu (0.39 × CI and 0.45 × CI, respectively) and low Sm (0.13 × CI) and Gd (0.17 × CI) abundances. The Y abundance follows that of the HREEs, but the remaining elements follow the trends shown by the other glasses. The contents of Cr and Li in Glass 5 are the lowest encountered.

Trace element abundances in minerals, all embedded in the glass of inclusion 2, vary over a wide range (Fig. 8). Apatite is the richest in trace elements with REE, Y, and Sr abundances between 94 × CI (Lu) and 360 × CI (La). The LREEs are enriched over the HREEs and Eu has a negative abundance anomaly, which is characteristic for all minerals in this inclusion. Other trace elements have low abundances: V and Cr < 0.01 × CI, Li ~ 0.02 × CI, Ti, Nb, and Mn ~ 0.3 × CI and Zr, Sc, and Ba at about chondritic abundance. Only Be and B (2.6 and 4.6 × CI, respectively) have elevated abundances. Clinopyroxene has a smooth REE abundance pattern with HREEs > LREEs (~10 × CI for Gd to Lu and ~1.5 × CI for La) and a negative Eu anomaly (~2 × CI). Clinopyroxene is also rich in Sc and Y (~10 × CI), and less so in Zr, Ti, Sr, Be, V, Cr, Mn, and Li, which have abundances between 1 × CI and ~5 × CI. Below chondritic abundances have B, Rb, Nb, and F at ~0.3–0.6 × CI and Ba at 0.01–0.02 × CI. Low-Ca pyroxene has a trace element abundance pattern that approximately follows that of the clinopyroxene, but at a much lower level and a steeper overall slope. The REEs range in abundance from 0.02 × CI (Ce) to 3.6 × CI (Lu) and form a smooth pattern with a negative anomaly for Eu and a positive one for La. Abundances of Sc, Y, Ti, V, Cr, Mn, and Li follow those of the HREEs (~1–4 × CI), those of Zr, Nb, Sr, Be, B, Rb, and F follow those of the LREEs (~0.07–0.4 × CI) and that of Ba is very low at 0.004 × CI.

Table 3. EMP analyses of phases from glass-rich inclusions in the Kodaikanal (IIE) iron (in wt%). Glass I1 is from inclusion 1, Glass I2 from inclusion 2, and Glass I3 from inclusion 3. Number of analyses in parentheses.

	CpxA(26)	CpxB (1)	Opx (11)	Glass I1 (7)	Glass I2 (15)	Glass I3 (16)	Chr (1)	Ap (1)
SiO_2	53.3	53.8	56.3	68.9	67.7	64.4	1.00	0.71
TiO_2	0.34	0.45	0.22	0.41	0.46	0.51	3.4	
Al_2O_3	1.23	1.20	0.37	17.8	19.4	18.9	9.8	
Cr_2O_3	1.28	1.43	0.45	0.14	0.20	0.15	50.2	0.02
FeO	5.5	4.7	10.4	0.48	0.82	1.19	27.6	0.45
MnO	0.30	0.24	0.51	0.13	0.17	0.18	0.66	
ZnO	0.04	0.03					0.06	0.05
MgO	18.0	17.0	31.1	0.10	0.08	0.13	6.0	0.18
CaO	18.9	20.5	1.30	0.10	0.21	0.16		54.2
Na_2O	0.50	0.73	0.08	4.1	6.8	7.1		0.06
K_2O				6.4	3.7	2.7		
P_2O_5		0.02	0.02	0.21	0.20	0.25	0.03	42.7
Cl				0.02				0.25
Total[a]	99.39	100.10	100.75	98.79	99.74	95.74	98.75	98.62

[a]Not corrected for O equivalent of Cl.
Cpx = clinopyroxene; Opx = low-Ca pyroxene; Chr = chromite; Ap = apatite.

Table 4. SIMS analyses of phases from Kodaikanal glass-rich inclusions (in ppm).

Element	Glass 1, incl.1	Error	Glass 2, incl. 2	Error	Glass 3, incl. 2	Error	Glass 4, incl. 1	Error
Li	7.34	0.04	0.492	0.009	1.68	0.02	6.55	0.04
Be	3.09	0.02	1.23	0.01	1.42	0.01	2.74	0.02
B	135.8	0.3	12.13	0.07	12.86	0.08	131.5	0.3
F	2.3	0.2	17.2	0.7	23.4	0.9	1.7	0.2
Na								
Mg	487	1	1083	1	1278	2	436	1
P	1545	3	1455	2	1487	3	1444	3
Cl	7.4	0.6	241	4	180	5	11	1
Ca	503.9	0.4			1386.4	0.8	481.3	0.4
Sc	4.52	0.07			2.98	0.06	4.12	0.07
Ti	2268	1	2370	1	2524	1	2200	1
V	3.18	0.04	6.24	0.05	5.68	0.06	3.02	0.04
Cr	67	0.2	6.66	0.06	6.73	0.07	33.8	0.2
Mn	101.3	0.3	148.8	0.3	173.6	0.4	93.8	0.3
Fe	2942	12	32,505	21	23,650	22	1890	6
Zn	518	7	1392	10	790	9	513	8
Rb	1136	2	497	1	928	1	1166	2
Sr	20.7	0.1	38.4	0.2	41.8	0.2	20	0.1
Y	2.25	0.04	1.92	0.03	2.2	0.04	2.18	0.04
Zr	45.1	0.3	44	0.2	45.8	0.3	43.3	0.3
Nb	52.5	0.3	4.26	0.07	5.38	0.09	50.6	0.3
Cs	42.6	0.4	31.4	0.3	27.1	0.3	44	0.4
Ba	17	0.2	21.2	0.2	19	0.2	16.3	0.2
La	0.1165	0.009	0.34	0.02	0.35	0.02	0.12	0.01
Ce	0.27	0.02	0.84	0.03	0.92	0.04	0.3	0.02
Pr	0.043	0.004	0.111	0.006	0.118	0.008	0.035	0.0035
Nd	0.2	0.01	0.42	0.02	0.46	0.02	0.2	0.01
Sm	0.057	0.006	0.106	0.009	0.1	0.01	0.058	0.007
Eu			0.08	0.01	0.09	0.01		
Gd	0.18	0.02	0.16	0.02	0.14	0.02	0.2	0.02
Tb	0.038	0.004	0.032	0.003	0.041	0.005	0.039	0.004
Dy	0.39	0.02	0.32	0.01	0.31	0.02	0.36	0.02
Ho	0.114	0.009	0.069	0.005	0.065	0.006	0.12	0.01
Er	0.39	0.02	0.227	0.009	0.25	0.01	0.36	0.02
Tm	0.057	0.005	0.036	0.003	0.035	0.004	0.055	0.005
Yb	0.25	0.02	0.23	0.01	0.2	0.02	0.17	0.02
Lu	0.092	0.008	0.045	0.004	0.052	0.006	0.073	0.007

Table 4. *Continued*. SIMS analyses of phases from Kodaikanal glass-rich inclusions (in ppm).[a]

Element	Glass-5, incl. 2	Error	OPX, incl. 2	Error	CPX-1, incl. 2	Error	CPX-2, incl. 2	Error	Ap, incl. 2	Error
Li	0.46	0.01	4.2	0.07	2.08	0.02	2.59	0.03	0.027	0.005
Be	1.5	0.02	0.011	0.001	0.053	0.002	0.064	0.003	0.064	0.006
B	19.7	0.1	0.23	0.02	0.61	0.02	0.44	0.02	4	0.2
F	6.4	0.6	3.2	0.3	34	1	16.7	0.9	38,700	150
Na			492	1	3617	2	3531	2	2140	5
Mg	670	2							1904	9
P	956	3	103	1	99.1	0.6	83.1	0.7		
Cl	35	3	11	2	113	3	65	3		
Ca	738.7	0.6	5689	4	121,365	64	124,800	80		
Sc	3.19	0.09	22.5	0.2	58.2	0.1	57.3	0.2	7	0.2
Ti	2199	1	1032	1	1840	1	1958	1	70	3
V	5.58	0.07	123.5	0.5	287.6	0.4	279	0.5	0.38	0.04
Cr	5.06	0.08	2972	3	9960	4	10,188	5	7	0.3
Mn	94.7	0.4	3648	4	2422	1.5	2321	2	567	3
Fe	5784	14	54,860	60	38,024	24	37,203	28		
Zn	386	8	377	12	2740	16	1856	16	188	13
Rb	758	2	0.36	0.08			0.66	0.25		
Sr	32.2	0.2	0.13	0.02	10.86	0.08	13.2	0.1	856	3
Y	0.46	0.02	2.3	0.07	13.82	0.08	15.5	0.1	330	2
Zr	36.7	0.3	0.25	0.02	4.68	0.08	5.5	0.1	5.5	0.5
Nb	5.2	0.1	0.018	0.004	0.12	0.01	0.13	0.02	0.08	0.01
Cs	38.8	0.5	0.16	0.03	0.15	0.01	0.15	0.02	1.5	0.2
Ba	11	0.2	0.009	0.004	0.025	0.004	0.044	0.006	2.3	0.3
La	0.093	0.009	0.016	0.004	0.3	0.02	0.39	0.02	84	1
Ce	0.2	0.02	0.012	0.002	1.65	0.04	1.84	0.06	217	2
Pr	0.024	0.003	0.005	0.001	0.36	0.02	0.43	0.02	27	0.6
Nd	0.084	0.007	0.039	0.004	2.42	0.06	2.81	0.08	152	2
Sm	0.02	0.004	0.024	0.004	1.26	0.05	1.32	0.07	46	2
Eu	0.08	0.01	0.0034	0.0009	0.106	0.007	0.13	0.01	5.9	0.3
Gd	0.034	0.008	0.09	0.01	1.91	0.09	2	0.1	44	2
Tb	0.009	0.002	0.033	0.004	0.33	0.02	0.39	0.03	8.3	0.5
Dy	0.057	0.005	0.28	0.02	2.58	0.07	2.78	0.08	52	1
Ho	0.016	0.002	0.085	0.009	0.45	0.02	0.55	0.03	10.2	0.5
Er	0.061	0.005	0.4	0.02	1.45	0.05	1.66	0.06	25.9	0.9
Tm	0.011	0.002	0.065	0.008	0.21	0.01	0.24	0.02	3.2	0.2
Yb	0.072	0.008	0.48	0.05	1.33	0.07	1.3	0.1	20	1
Lu	0.011	0.002	0.09	0.01	0.22	0.02	0.21	0.02	2.3	0.3

[a]OPX = low-Ca pyroxene; CPX = clinopyroxene; Ap = apatite.

DISCUSSION

Problems with Magmatic and Impact Origins for Some Iron Groups

In the following paragraphs, we discuss some of the data that are in conflict with the widely accepted model that iron meteorites are made of metal that crystallized from a metal melt.

One problem is posed by the fact that the chemical groups of the iron meteorites, each believed to represent a single planetary core, apparently followed different rules in local fractionation processes (as indicated by individual and widely different slopes in two-element correlation plots, e.g., Ir versus Ni plots, indicating different elemental solid-liquid distribution coefficients). Possible explanations for this behavior require ingeniously complex models (e.g., Wasson 1985; Haack and Scott 1992; Jones and Malvin 1990). Furthermore, because metal is a good heat conductor, irons from one and the same core should have very similar cooling rates, which is not observed. For example, IVA irons, among others, display widely different individual cooling rates (e.g., Rasmussen et al. 1995; Haack et al. 1996). In addition, given the very high melting temperatures and generally very low cooling rates estimated for irons, the metal within a given meteorite should be chemically homogeneous, which is not the case in the Canyon Diablo IAB, the Campo del Cielo IAB, and the Acuña IIICD irons (e.g., Wasson 1968; Kurat et al. 1991, 2000). A special problem is also posed by common schreibersites included in metal. Their chemical compositions (and trace element contents) are highly variable and correlated with the size of the crystals (Jochum et al. 1980;

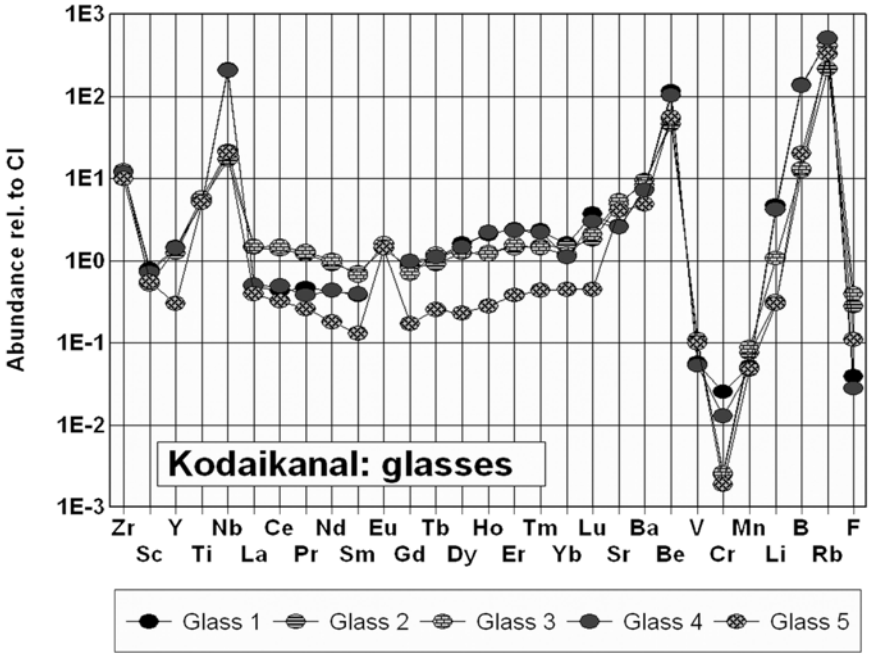

Fig. 7. CI-normalized trace element abundances in glasses from silicate inclusions of the Kodaikanal IIE iron. Glasses 1 and 4 are from the glass-only inclusion #1, Glasses 2 and 3 co-exist with pyroxenes, and Glass 5 co-exists with apatite in inclusion 2.

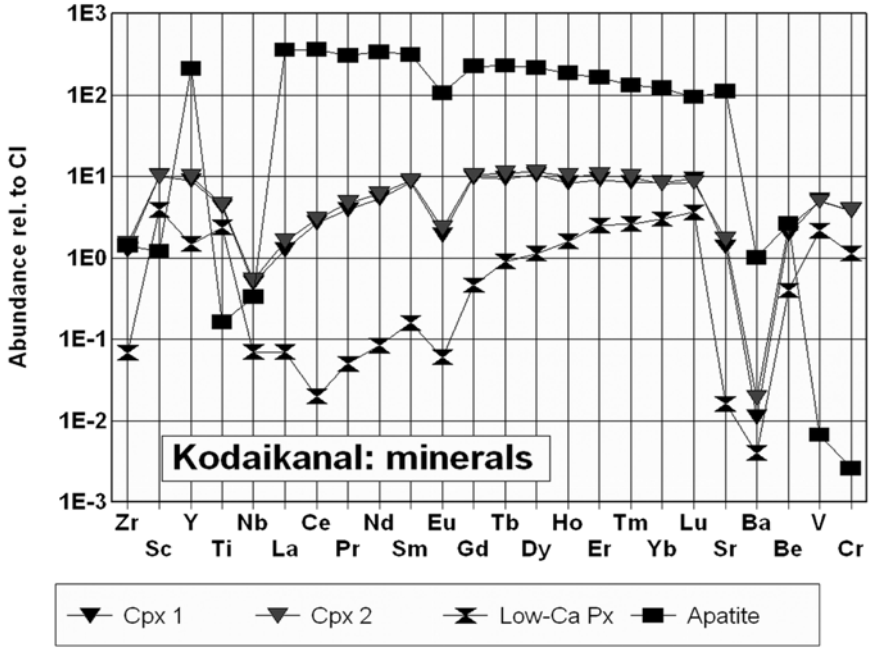

Fig. 8. CI-normalized trace element abundances in minerals from silicate inclusion 2 of the Kodaikanal IIE iron. Cpx = clinopyroxene; low-Ca Px = low-Ca pyroxene.

Skala et al. 2000; Kurat et al. 2002a) and this in spite of the very low apparent cooling rates, which, however, were not low enough to achieve chemical equilibration between schreibersites and between schreibersites and metal. A compositional zoning is expected to develop but is not detectable (Clarke and Goldstein 1978). Isotopic disequilibrium in irons is also widespread. Graphite has widely variable C isotope compositions on a small scale (Deines and Wickman 1975; Maruoka et al. 2003). Nitrogen isotopic ratios are also variable in metal and other phases of irons (e.g., Franchi et al. 1993; Sugiura 1998; Asame et al. 1999).

Another problem is posed by the apparent radiogenic ages of metal and of inclusions in irons meteorites. Recently, it was found that metal of iron meteorites has a deficit in the radiogenic isotope ^{182}W, daughter of short-lived ($T_{1/2}$ = 9 Myr) ^{182}Hf, as compared to chondrites, indicating siderophile-lithophile element separation very early in the solar system (Harper and Jacobsen 1996; Quitte et al. 2000; Schersten et al. 2006). If applied to the common genetic model of iron meteorites, this fact would make the irons the oldest objects of the solar system. Given that the common chondritic inclusions in irons have ages indistinguishable from those of chondrites or are even younger (Burnett and Wasserburg 1967; Snyder et al. 2001), this is a physical impossibility. However, irons (or their precursors) must be old not only because of their primitive W, Pb, and Re/Os isotopes (Birck and Allegre 1998), but also because they contain carriers of primitive gases (e.g., Asame et al. 1999; Matsuda et al. 2005) and they contain daughters of now-extinct radionuclides. So far, ^{129}Xe (e.g., Alexander and Manuel 1968; Bogard et al. 1969, 1971; Niemeyer 1979; Meshik et al. 2004), ^{107}Ag (Chen and Wasserburg 1983; Kaiser and Wasserburg 1983), and ^{53}Cr (Sugiura and Hoshino 2003) excesses have been reported.

Also, common silicate inclusions in IAB and IIICD irons, which are supposed to have been picked up by the metal melt, do not exhibit any sign of force (or shock features) nor any sign of heat: neither the silicates not the metal plus sulfide were heated to the minimum eutectic melting temperature—a physical impossibility considering the very small sizes of some of these inclusions (for excellent descriptions, see Bunch et al. 1970). The same holds for the preservation of delicate aggregation and growth structures of inclusions in irons (e.g., El Goresy 1965; Kracher 1974; Nehru et al. 1982).

In spite of the very low cooling rates indicated by the metal, the silicates and oxides are usually chemically out of equilibrium. In addition, glassy objects and glass inclusions are very common and give clear evidence for quenching rather than slow cooling. The latter should have led to devitrification and recrystallization of the glasses into equigranular metamorphic rocks. The presence of glasses is another strong argument against mixing of the silicates with a metal melt. Rather, all evidence points toward a subsolidus deposition of metal in a gentle process that preserved highly delicate textures, chemical and isotopic disequilibria, and even glasses (see Kurat 2003).

Our results, as discussed below, are also in conflict with formation of irons from a melt, and therefore we have to question the validity of this model.

The Problem of Silicate Inclusions in IIE Irons

Silicate inclusions in IIE irons are highly diverse in their texture, mineralogy, and chemical composition. The Rb-Sr ages are also variable, ranging from fairly high (e.g., Colomera, 4.51 Ga) (Sanz et al. 1970) to fairly low (e.g., Kodaikanal, 3.5–3.7 Ga) (Burnett and Wasserburg 1967; Bogard et al. 1967). This diversity (e.g., Bunch et al. 1970; Casanova et al. 1995) has motivated researchers to formulate several genetic models. However, one feature is common to all silicate inclusions in IIE irons: they kept a memory of a chondritic source because they have oxygen isotopic compositions that are similar to those of H chondrites (Clayton et al. 1983). Because of this property, all genetic models of IIE irons involve collision of (molten or solid) metal with or impact into a target of H chondritic composition (e.g., Wasson and Wang 1986; Ruzicka et al. 1999, 2006; Hsu 2003; Takeda et al. 2003).

However, our data on Guin and Kodaikanal inclusions in part support existing models but are also in conflict with them. This begins with the fact that the composition of the low-Ca pyroxene encountered in Kodaikanal inclusion 2 roughly fits the composition of equilibrated H chondrite orthopyroxene, whereas the composition of the clinopyroxene indicates an affinity with L chondrites. In addition, there are no traces of shock (e.g., crushing, polysynthetic twinning, kink bands, planar features, recrystallization, isotropization, selective melting, etc.) in the silicates we studied, minerals and glasses are out of chemical equilibrium, and the distribution of elements between phases is inconsistent with an equilibrium process. All this is discussed in the following paragraphs and an attempt is made to find an explanation for the situation encountered.

Mineral Compositions

There apparently exists a weak link between IIE silicate inclusions and H chondrites (as also suggested by the O isotopes) (e.g., Clayton et al. 1983): the low-Ca pyroxene in Kodaikanal inclusion 2 (Table 3) has a major and minor element composition similar to that of orthopyroxene from equilibrated H chondrites, but with an FeO content at the lower end of the range (10.4 wt%) and TiO_2, Al_2O_3, and Cr_2O_3 contents somewhat high, up to about twice those of H chondrite pyroxenes (all comparison data are from Brearley and Jones 1998). The clinopyroxene in inclusion 2 has a composition comparable to that of clinopyroxene from ordinary chondrites—similar to those from L chondrites (TiO_2, FeO, MnO, Na_2O)—but has too much Al_2O_3 (1.23 versus 0.3–0.8 wt%), too little CaO (18.9 versus 20–22.5 wt%) and has no similarity with clinopyroxene from H chondrites. Chromite has a composition outside the range for ordinary chondrite (OC) chromite with low FeO (28 versus 30 wt%) and Cr_2O_3 (50 versus >55 wt%) and high Al_2O_3 (9.8 versus ~6 wt%). Such a composition is known from unequilibrated OCs (Wlotzka 2005), notably from Mezö-Madaras (e.g., Hoinkes and Kurat 1974).

Pyroxenes and chromite in Kodaikanal appear to have been derived from a chondritic source or have experienced

processes similar to those experienced by the constituents of chondrites. The affinity appears to be with OCs, somewhere between H chondrites (low-Ca pyroxene) and L chondrites (clinopyroxene). The phases are out of chemical equilibrium with each other (e.g., Fe-Mg distribution between crystals and trace element distributions between crystals and glass) (see distribution coefficients listed by Green 1994 and discussion below), probably as a consequence of incomplete metasomatic elemental exchange between silicates and the solar nebula, a feature very common among all meteorites (e.g., Kurat 1988).

Mineral-Glass Relationship

Pyroxenes, chromite, and apatite in Kodaikanal have euhedral, commonly skeletal habits and are embedded in devitrified glass. Apparently, these phases crystallized from a liquid that was quenched to glass. However, when looking at the chemical composition of the glass, it becomes clear that a liquid of such chemical composition could never have produced the mineral phases the glass now carries. It is extremely poor in Cr, Mn, Mg, and Ca but very rich in Si, Na, and K. The overall chemical composition resembles that of glasses in enstatite meteorites (e.g., Keil et al. 1989), in Chassigny (a SNC olivinite) (Varela et al. 2000), ALH 84001 (a SNC pyroxenite) (Kurat et al. 1997), and in some terrestrial upper mantle peridotites (e.g., Varela et al. 1998). Characteristically, all of these glasses have very high alkali contents ($Na_2O + K_2O$ commonly >10 wt%) and high SiO_2 contents (~65–80 wt%), and Na_2O/K_2O ratios that are around unity—far removed from the chondritic value. Thus, we have a highly curious situation with apparently chondritic silicates and chromite (belonging to different chondrite clans) being enclosed by a former liquid that is totally out of equilibrium with these phases and in addition that shows extreme chemical fractionation. This looks like a physical impossibility, especially because the minerals have crystal habits that indicate crystallization from the liquid in which they are trapped.

The low-Ca pyroxene of Kodaikanal inclusion 2 is a good example of a reaction product from a phase (the Ca-rich pyroxene) not in equilibrium with the enclosing liquid (Fig. 5b). Apparently, Ca was removed from the system, making the augite unstable. As a consequence it broke down and reacted with the liquid to form low-Ca pyroxene:

$$CaMgSi_2O_6(s) \rightarrow MgSiO_3(s) + SiO_2(l) + CaO(l) \quad (1)$$

(s = solid; l = dissolved in liquid)

The CaO liberated in this way from augite is no longer traceable in the glass, and so must have had a sink where it was needed urgently. A possible sink could have been the phosphates, which are abundant and located preferentially near the inclusion's surface, which indicates that P_2O_5 was added to the liquid from the environment and caused the augites to become unstable. While this happened, the liquid still had high trace element contents because all phases, the original augite, and the secondary low-Ca pyroxene and phosphates are rich in trace elements and indicate derivation from a liquid with about 10–50 × CI trace element abundances (see discussion below).

The new stable phase formed; the low-Ca pyroxene, however, is also out of equilibrium with a liquid of the composition of the glass it is in contact with, but shows no sign of any reaction with that liquid. This fact has also been recognized by former studies of silicate inclusions in IIE irons (e.g., Ruzicka et al. 1999, 2006; Hsu 2003; Takeda et al. 2003). The major element abundance evolution of such liquids has been discussed in great detail by Ruzicka et al. (1999) and this discussion need not be repeated here. These authors reached a clear conclusion: "the large scatter and lack of systematic relationships for IIE inclusions suggest that they were not differentiated in the same way as terrestrial volcanic rocks. In particular, their varied compositions appear to reflect processes other than simple partial melting or fractional crystallization." (p. 2130). However, this clear and strong conclusion did not generate new genetic models for IIE silicate inclusions. Most workers in this field keep propagating the impact model (FeNi impactor—chondritic or differentiated target), a model highly popular among meteoriticists, without defining the differentiation mechanism in detail. Very recently, Ruzicka et al. (2006) were also faced with that problem in their study of silicate inclusions in the Sombrerete ungrouped iron meteorite and suggested a solution via a "filter-press fractionation" process, "in which liquidus crystals of Cl apatite and orthopyroxene were less able than silicate melt to flow through the metallic host between inclusions. This process enabled a phosphoran basaltic andesite precursor liquid to differentiate within the metallic host, yielding a dacite composition for some inclusions." We do not see a possible application of that process for our inclusions in Guin and Kodaikanal, mainly because:

- a partial melt from a chondrite cannot have exclusively apatite and low-Ca pyroxene at its liquidus—it needs to be saturated with all phases present in chondrites;
- the bulk compositions of the liquids have no relationship to those of "andesites" or "dacites," especially in their trace element contents (and, consequently, should not be called "andesitic" and "dacitic");
- the fractionation of the alkali elements from chondritic proportions to highly fractionated proportions cannot be achieved that way—as is discussed below.

Most studies leave the problem of the alkali fractionation open, except the studies by Takeda et al. (2003) and Ruzicka et al. (2006), who discussed this problem in great detail. Takeda et al. (2003) recognized that fractionation of the alkalis is difficult and cannot be achieved via feldspars (see early discussion of that problem by Wlotzka et al. 1983 and

Kurat et al. 1984). Other mineral systems are needed and Takeda et al. (2003) concluded that "the K-rich material may have originated as a fluid phase that leached K from surrounding materials and segregated by a mechanism similar to that proposed for the Na-rich inclusions." This is indeed a process that has been identified in the formation of partial melts in the Earth's upper mantle with major element compositions similar to those of glasses in IIE irons. There, halogenites and carbonates appear to be responsible for these fractionations (e.g., Navon et al. 1988; Litvin and Zharikov 1999; Sokol et al. 2000; Varela et al. 1998). Ruzicka et al. (2006) don't see such difficulties and simply state their strong belief that "K-glass and Na-glass also formed by immiscible separation of a melt with an intermediate composition . . ." However, this seems to be a very unlikely process because silicate melts with much higher alkali contents than those involved in Sombrerete silicate inclusion formation also show perfect miscibility (e.g., Tuttle and Bowen 1958) and a silicate melt containing a few wt% of alkali oxides with a chondritic Na/K ratio (i.e., very low K content, type 1 inclusions in Sombrerete) has never been shown to tend to break down into Na-rich and K-rich melts.

Na-K fractionation is very common in constituents of E, LL, and L chondrites (e.g., Kurat 1967; Wlotzka et al. 1983; Kurat et al. 1984; El Goresy et al. 1988) and can have a variety of causes. As there seems to be a connection between LL chondrites and E meteorites (e.g., Kurat et al. 1984), fractionation via alkali sulfides, which, like halogenites, do not form Na-K solid solutions, is one possible way. These sulfides aggregate in different proportions (thus defining the Na/K ratio), are subsequently oxidized, and the alkalis dissolve in silicate liquids or diffusionally replace Ca in glasses (e.g., Kurat 1988; Varela et al. 2005). Many meteoritic objects appear to have formed that way—see good examples in the Krähenberg (Wlotzka et al. 1983) and Chainpur LL chondrites (Kurat et al. 1984). They contain alkali-rich glasses, which still carry relictic sulfides (now converted into troilite). Furthermore, the glass of Guin apparently was associated with and subsequently separated from sulfides as is evidenced by the incomplete disentanglement between sulfide and liquid at the former liquid's surface and the many tiny Fe/S-rich droplets in the Guin glass (Figs. 2a–c) that did not reach the surface because the time available was apparently too short for a clean separation.

A formidable problem is posed by the chemical composition of the glasses. Liquids of such composition are unable to crystallize the clinopyroxene and low-Ca pyroxene, which, however, are there, embedded in the glass and have obviously grown from that liquid, which became the glass by quenching. Takeda et al. (2003), Ruzicka et al. (2006), and other investigators do not address this problem in detail, although all investigators recognize the non-equilibrium situation: "Evidently, the analyzed glass did not form from a melt in complete equilibrium with either the analyzed orthopyroxene or merrillite" (Ruzicka et al. 2006). However, no explanation is given.

We offer a new solution to the conundrum posed by the euhedral crystals in a glass that bears no obvious chemical relationship to the crystals. When looking at Figs. 5 and 6, there cannot be any doubt that pyroxenes and apatite crystallized from the liquid that is now present as glass. However, that liquid, in order to be capable of crystallizing these phases, must have had a chemical composition that was very different from the one we now find for the glass. In particular, it must have contained 10–100 times the amount of REEs of the glass. Consequently, the glass must have changed its chemical composition after the crystals precipitated. The change, of course, must have taken place at sub-solidus temperatures, involving the glass and not the liquid, because the latter would have quickly reacted with the crystals, which are out of chemical equilibrium with the glass. Such a liquid-solid reaction is documented by the low-Ca pyroxene overgrowths on Ca-rich pyroxenes but is not preserved in the trace element abundances. Apparently, we see evidence for a change of the major element composition of the liquid that caused the reaction of Ca-rich pyroxene to form Ca-poor pyroxene. However, the trace element distributions between crystals and glass give clear evidence for an additional subsolidus metasomatic event that further changed the chemical composition of the glass (and likely also that of the crystals to some extent, e.g., adjustment of the Fe/Mg ratio). This is not an unusual situation for meteoritic objects, many of which comprise nonequilibrium phase associations that have been established by subsolidus metasomatic elemental exchange between the objects and the local solar nebula (e.g., Kurat and Kracher 1980; Peck and Wood 1987; Kurat 1988; Kurat et al. 2002b; Varela et al. 2003, 2005, 2006)—a simple consequence of nebular cooling (e.g., Fegley 2000). The uniform chemical composition of the pyroxenes is also a consequence of metasomatic elemental exchange—directly comparable with the uniform chemical compositions of Fe/Mg silicates in equilibrated ordinary chondrites (Keil and Fredriksson 1964) and other rocks (see discussion by Kurat 1988). This exchange is a process now well established experimentally and theoretically (e.g., Dohmen et al. 1998; Dohmen and Chakraborty 2003).

Glass Composition and Geochemical Fractionation

All glasses investigated by us have strongly fractionated trace element contents (Fig. 9)—as can be expected from the fractionated major element abundances. They display a peculiar feature, which is also evident in the major element abundances: some incompatible elements (e.g., Ti, Nb, B, Rb) are strongly enriched over the compatible ones—as they should be—but others, notably the REEs, are not. Apparently two fractionation processes were active:

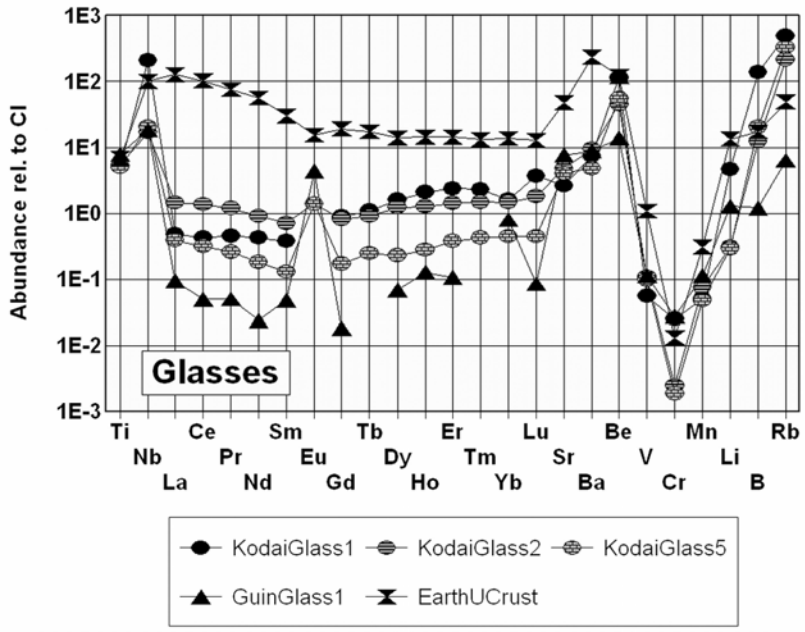

Fig. 9. CI-normalized trace element abundances in glasses from silicate inclusions in Guin (UNGR) and Kodaikanal (IIE) irons and in the Earth's upper crust (from Taylor 1992). All glasses have very low REE contents but are rich in some other incompatible elements. The abundance patterns of the glasses are very different from that of the Earth's crust and thus indicate fractionation by processes different from geochemical processes.

- a geochemical (crystal-liquid) fractionation that led to the enrichment of incompatible elements (Ti, Nb, Sr, Ba, Be, B, Rb) and the depletion of compatible elements (V, Cr, Mn, Li) in the liquid;
- an independent fractionation of the REEs, possibly by extraction of REEs from the system.

The depletion of the REEs in the glasses is very pronounced, with their abundances being as low as 0.01–1 × CI. The chemical composition of the glasses is thus far removed from those rocks they are commonly referred to: terrestrial rhyolites, dacites, and andesites. Comparison with the andesitic terrestrial crust (Fig. 9) reveals that the Guin and Kodaikanal glasses have seen fractionation processes that were very different from those taking place in the Earth's planetary crust (and others).

Ruzicka et al. (2006) fractionate the REE contents by extracting varying amounts of phosphates in a "filter-press differentiation process" where liquids can move through (partly liquid!) metal, but crystals cannot. They state: "trace-element data strongly suggest that glass became depleted in those elements that were sequestered in Cl apatite and merrillite . . ." However, in reality, the glasses are so poor in REE that they could never have been in equilibrium with phosphates, which are very rich in REEs (see discussion on apatite-glass relationship below). To explain this situation, crystal-liquid distribution coefficients would be needed having values never observed in nature or in experiments (e.g., Green 1994; Prowatke and Klemme 2006).

Not only are the low abundances of the REEs peculiar, but also their abundance patterns are as well, none of which follow the geochemical fractionation trend toward LREEs > HREEs. The patterns are either flat, V-shaped, or even HREE-enriched. Consequently, the glasses could not have seen a process like terrestrial geochemical elemental fractionation.

The flat patterns apparently document nongeochemical fractionation of the REEs from other elements, a depletion by indiscriminate removal of REEs. This can be done by removal of either a REE-rich phase with flat abundance pattern or a vapor from the system. As the system apparently was not dominated by a liquid (which would force a geochemical fractionation), a vapor fractionation is indicated. This view is supported by two additional features of REE patterns in the glass: the HREEs > LREEs abundances in Kodaikanal Glass 1 and 4 and the abundance anomalies for Eu and Yb (positive and negative). Anomalies in the abundances of Eu are common in extraterrestrial and terrestrial systems and are due to the easily achieved reduction of Eu^{3+} to Eu^{2+}, which follows Ca^{2+} into the structure of plagioclase. Also, Yb can be reduced to Yb^{2+}, but its ionic radius does not allow it to follow Eu^{2+} into the Ca-Al-silicate lattices (e.g., Strange et al. 1999). Therefore, anomalies in Yb abundances are usually attributed to cosmochemical (nebular) fractionations because Yb has—like Eu—a lower condensation temperature than the rest of the REEs (e.g., Lodders 2003). Indeed, Eu and Yb depletions are very common in highly refractory phases of CAIs (e.g., Ireland et al. 1988; Fahey et al. 1994). They are frequently accompanied by a REE abundance pattern with

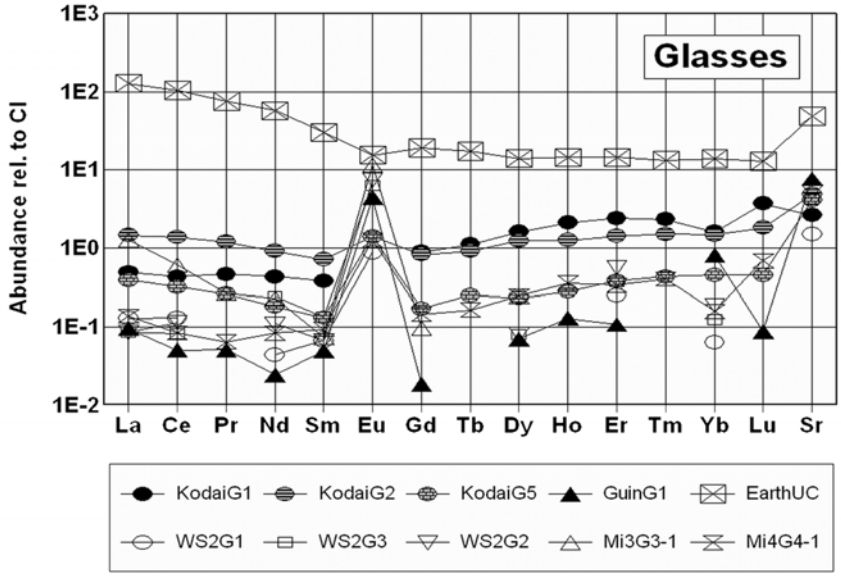

Fig. 10. CI-normalized REE and Sr abundances of glasses from Kodaikanal (IIE), Guin (UNGR), Weekero Station (IIE), Miles (IIE) irons, and the Earth's upper crust (data from Ruzicka et al. 1999; Hsu 2003; Taylor 1992). There is a 100-fold range in normalized REE abundances but at very low abundance level as compared to a fractionated solar system planetary crust, which has 100–1000 times higher La abundance than the IIE iron glasses.

HREEs > LREEs, a consequence of the fact that condensation temperatures of the HREEs are higher than those of the LREEs. Kodaikanal Glasses 1 and 4 have such an ultrarefractory pattern in spite of the fact that they are strongly depleted in total REEs and are strongly enriched in volatile alkalis compared to ultrarefractory phases from CAIs (e.g., Fahey et al. 1994). Possibly, we see an admixture of a small amount of an ultrarefractory phase to that liquid.

A contrasting pattern with very low REE and positive Eu and Yb anomalies is exhibited by the Guin Glass 1. It apparently documents a condensate from a system from which the most refractory REEs have almost completely been removed. The co-existing apatite carries the complementary trace element signature of this phase, which, not being a refractory mineral phase, is likely to be a derivative of such a phase (see discussion below).

Glasses from other IIE irons have major, minor, and trace element contents similar to those found in the Kodaikanal and Guin inclusions (Fig. 10). However, a strong positive Eu abundance anomaly seems to be common and is occasionally accompanied by a small negative Yb anomaly. There have been several attempts to explain this feature by geochemical fractionation. Hsu (2003) discussed this at length and had to admit that "the origin of Yb anomalies in IIE silicate inclusions remains unsolved." Takeda et al. (2003) also discussed this problem and concluded that "This indicates that Yb fractionation was somehow related to mixing of the crystal mush with molten metal" and "negative Yb anomalies might have been produced by evaporation under reducing conditions." Ruzicka et al. (2006) describe positive Yb and Sm abundance anomalies in phosphates of Sombrerete and suggest "that the positive anomalies in phosphate formed as a result of gas-melt-phosphate partitioning." Their suggestion implies that in the presence of a vapor phase the phosphate does not obey the crystal-liquid distribution coefficients and thus depletes the "glass" by enriching itself in these elements ("3-phase partitioning effects"), a physically unlikely process. The authors also recognize the necessity of reducing conditions during the formation of Yb and Sm anomalies and also recognize that the presence of phosphates and the high Fe/Mg of the silicates indicate the opposite. As a solution, Ruzicka et al. (2006) suggest that the "phosphate-melt-gas partitioning" took place "under highly reducing conditions; such a gas would have been present momentarily at the start of inclusion crystallization." However, this idea does not take care of the fact that the evidently oxidized phosphates are the liquidus phase over a large range of temperatures.

The geochemical fractionation and the evaporation models of Hsu (2003) and Takeda (2003) are at odds with the very low abundances of the REEs and—as we know from our study—the high abundances of some incompatible elements, among them highly volatile elements like Na (50% condensation temperature; CT 958 K; all taken from Lodders 2003), K (CT 1006 K), Rb (CT 800 K) and B (CT 809 K). Their high abundances practically exclude the possible evaporative loss of Yb because all these elements should have been lost completely. We suggest that all patterns can be made by fractional condensation because the 50% condensation temperatures for Eu and Yb are quite different at 1356 and 1487 K, respectively (Lodders 2003), but are much higher than those of the volatile elements Na, K, Rb, and B. The CT

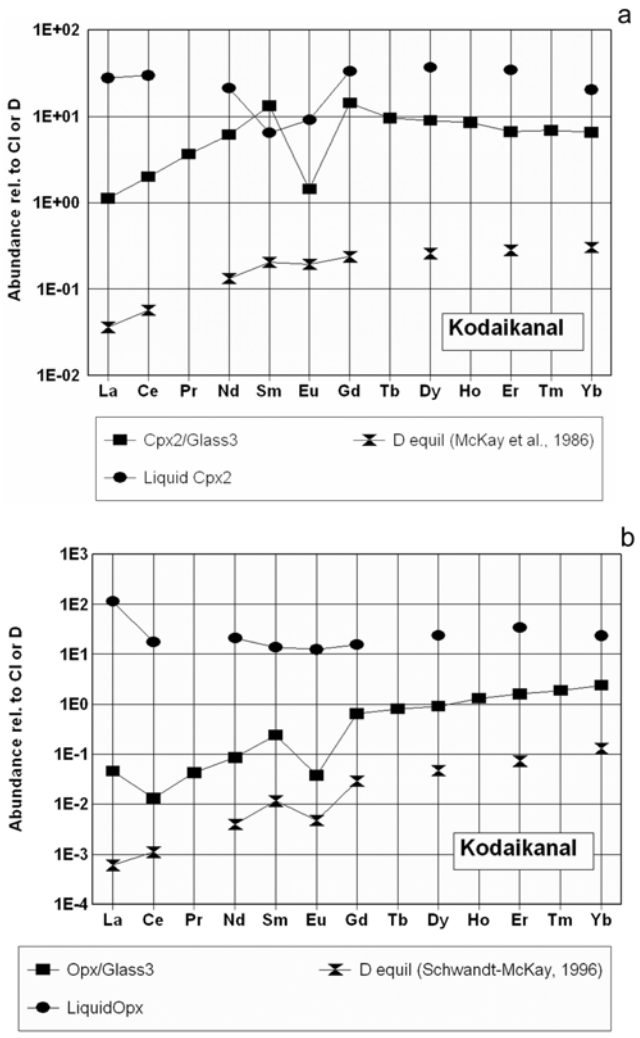

Fig. 11. CI-normalized estimated liquid compositions in equilibrium with clinopyroxene (a) and low-Ca pyroxene (b) in Kodaikanal inclusion 2. Also plotted are the Kd (px-l) used (McKay et al. 1986; Schwandt and McKay 1996) and the distribution of REEs between minerals and glass as observed (px/glass abundance ratios). Pyroxenes are obviously far out of equilibrium with the glass they are immersed in and indicate derivation from a melt with 10–40 × CI REE abundances. The high La value for the low-Ca pyroxene is likely due to contamination with glass.

of Yb being higher than that of Eu makes it unlikely that Yb can be lost in an evaporation event without loss of Eu, which, however, is strongly enriched over Yb. It is curious that the straightforward explanation for the Yb anomaly via condensation, which is widely accepted for CAIs and chondrules, appears to be unacceptable for inclusions in irons—and this in spite of the fact that irons have been identified as being one of the most ancient objects of the solar system (see, e.g., Schersten et al. 2006).

The strong depletion of Mg/Fe-silicate–compatible elements (V, Cr, Mn) in all glasses from Kodaikanal and Guin could be an indication for a fractionation via Mg/Fe silicates (precipitation of such silicates from the liquid) and also possibly via a metal phase because all three elements can be siderophile/chalcophile under reducing conditions. However, the possibility of vapor fractionation is left as an alternative for Cr and Mn because these elements are moderately volatile and usually depleted with respect to the refractory elements in, e.g., chondrules and aggregates of CV and CM chondrites (e.g., Varela et al. 2005, 2006).

Mineral Glass Disequilibria

The chemical compositions of glasses in Guin and Kodaikanal (as well as other IIE irons) are not only unusual but are also apparently unrelated to those of the mineral phases they carry. This has been recognized by all students of IIE iron inclusions (e.g., Bunch et al. 1970; Ruzicka et al. 1999, 2006; Hsu 2003; Takeda et al. 2003) and discussed in great detail. However, no satisfactory explanation has been offered so far. All models utilize mixing of minerals, fractionated melts, and molten metal in planetary impact events. In these models, augite, low-Ca pyroxene, and apatite must have crystallized in a foreign system and were trapped by the shock-melted plagioclase-quartz mixture. However, minerals are commonly phenocrysts in the glass, indicating in situ crystallization and glasses are enriched in elements that cannot have been derived from plagioclase or quartz (see above) and are depleted in the plagiophile elements such as the LREEs. Below we discuss briefly the mineral-glass disequilibria encountered in Guin and Kodaikanal and offer a new solution of the problems posed.

Pyroxene-Glass Relationship

As discussed above, the pyroxenes in Kodaikanal inclusion 2 appear to have grown from the liquid in which they are now trapped (euhedral and skeletal crystals in glass), but that liquid could not have had the chemical composition the co-existing glass now has. The pyroxenes are obviously far out of equilibrium with the glassy mesostasis. Abundances of REEs in a liquid in equilibrium with the clinopyroxene and orthopyroxene in Kodaikanal inclusion 2 (Figs. 11a and 11b) would need to be between about 10 × CI and 40 × CI. That is very different from what we observe in the glass in contact with the pyroxenes in this inclusion (REE abundances of around 1 × CI; see Fig. 7). Similar disequilibria have been described for silicate inclusions of Miles and Weekeroo Station and prompted the proposal that the feldspathic glass could have formed by remelting of pre-existing feldspar and pyroxene (Ruzicka et al. 1999) or feldspar, pyroxene, and tridymite (Hsu 2003). Although some match of the REE patterns with those of the glasses can be obtained by these mixtures, three important features cannot be matched. First, the highly fractionated Na_2O/K_2O ratio of the glasses (as discussed above) is clearly impossible to achieve by melting of H chondrite feldspar and pyroxene and needs a

fractionation mechanism that involves nonsilicates. Second, the combination of high concentrations of some incompatible elements with low concentrations of REEs in the glasses can also not be achieved this way. Concentrations of Zr, Ti, Nb, Sr, Ba, Be, K, Na, and Rb—all around 10 × CI in Guin and Kodaikanal glasses and occasionally reaching >100 × CI (Nb, Be, and Rb in Kodaikanal glass)—combined with REE abundances of 0.01 to 2 × CI cannot be achieved in this way. Third, many glasses and also pyroxenes have a negative Yb abundance anomaly (e.g., Hsu 2003; Takeda et al. 2003; Ruzicka et al. 2006), which cannot be explained by either shock or partial melting. This anomaly is also present in our sample and is accompanied by a negative Eu anomaly in Kodaikanal glassy inclusion 1 (as it is also in pyroxenes in Colomera [Takeda et al. 2003]).

Clearly, pyroxenes crystallized from a liquid that subsequently was quenched to glass. The chemical mismatch between the minerals and the glass can only be explained by changing the chemical composition of the glass after formation of the assemblage. A metasomatic process is indicated; we shall discuss this below.

Apatite-Glass Relationship

Apatite in Guin and in Kodaikanal is very rich in the REEs, Y, and Sr (Figs. 3 and 8), which is very different from the co-existing glass (Figs. 3 and 7). The complementary REE patterns of apatites in Guin and Kodaikanal and the co-existing glass at first sight suggest an igneous origin. However, compared to experimental distribution coefficients of the REEs and other trace elements between apatite and a siliceous liquid (e.g., Green 1994; Prowatke and Klemme 2006), the apatite-glass assemblages are far out of equilibrium (e.g., La Kd ~ 11.4, but $La_{[ap]}/La_{[gl]}$ ~ 740–915), except for Sr. In addition, the REE abundance pattern of apatite does not follow the distribution coefficients (having a hump with La < Sm > Lu), but rather is flat. A hypothetical liquid from which apatite could have been crystallized would need to have REE abundances of about 20 × CI in Kodaikanal and ~5 × CI in Guin (Fig. 12), in the latter case with a pattern complementary to that of the distribution coefficient (La > Sm < Lu). This suggests that the Guin apatite did not grow from a liquid, which is supported by its location at the surface of the glass and by its grain size and shape. However, the occurrence and habit of apatite in Kodaikanal glass give clear evidence for in situ crystallization from a liquid. In addition, the composition of the hypothetical liquid in equilibrium with that apatite is similar to those calculated for liquids in equilibrium with the pyroxenes, which also have igneous habits and occur within the same inclusion. Thus, all three major phases present in inclusion 2 glass indicate derivation from a liquid that was rich in refractory trace elements at a level of about 10–40 × CI. Interestingly, such liquids are commonly involved in meteorite formation, have been dubbed by us as "universal liquid" (e.g., Varela and Kurat 2004, 2006; Varela et al. 2005, 2006) and seem to be responsible for the formation of a rich variety of objects, such as single olivine crystals, chondrules and aggregates, pyroxenites (diogenites), eucrites, angrites and many more. It is apparent that traces of the action of a primary solar nebula liquid exist also in silicate inclusions of iron meteorites.

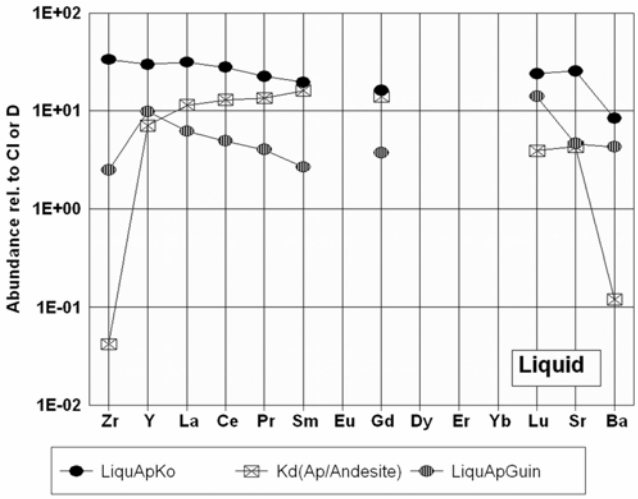

Fig. 12. CI-normalized estimated liquid trace element contents in equilibrium with apatite in Kodaikanal and Guin silicate inclusions and partition coefficients used (Prowatke and Klemm 2006).

The trace element abundances and the pattern of the Guin apatite do not fit the primary nebula liquid system and indicate a genesis different from that of the Kodaikanal apatite. The Guin trace element abundance pattern rather resembles the group III pattern of CAIs (Martin and Mason 1974) at an abundance similar to that found in hibonites (e.g., Ireland et al. 1988) and oldhamites (e.g., Kurat et al. 1992; Crozaz and Lundberg 1995). The pattern and abundance level suggest a trace element–rich precursor phase of the apatite that formed by condensation from nebular gas at low fO_2 (Lodders and Fegley 1993). Oldhamite is probably the best guess as it can be easily transformed into apatite by oxidation. First, CaS is oxidized (it actually should burn):

$$2CaS(s) + 3O_2(g) = 2CaO(s) + 2SO_2(g) \quad (2)$$

(s = solid; g = gas)

Then the lime produced reacts with gaseous species of P and Cl to produce apatite:

$$10CaO(s) + 3P_2O_5(g) + 2Cl(g) = 2Ca_5(PO_4)_3Cl(s) \quad (3)$$

$P_2O_5(g)$ can be obtained from the cooling vapor—as indicated by the destabilization of augite in Kodaikanal inclusion 2—or from the burning of schreibersite, barringerite, perryite, or any other phosphide, if necessary:

$$4(Fe,Ni)_3P(s) + 5O_2(g) = 4(Fe,Ni)(s) + 2P_2O_5(g) \quad (4)$$

Perryite could in addition also contribute to the high SiO_2 content of the glasses.

The co-existence of oldhamite and silica-alkali–rich glass is also typical for enstatite meteorites (e.g., Keil et al. 1989; Varela et al. 1998). In addition, the complementary REE patterns of apatite and glass in Guin indicate that these phases are related: the removal of REEs from the local vapor by the apatite precursor could have created the REE-depleted but Yb and Eu-enriched environment necessary for the formation of the REE-poor liquid which was quenched to glass. This is a possible explanation for Guin but a different mechanism for the removal of REEs from the glass is needed for Kodaikanal. Possibly, a metasomatic process that removed Ca, Mg, and Fe from the glass is also responsible for the removal of the REEs, which found a sink outside the glass—possibly they became concentrated in an REE-rich phase such as that present in OC chondrite matrices (e.g., Rambaldi et al. 1981).

Rutile-Glass Relationship

Rutile in the Guin inclusion is generally poor in trace elements, in particular in REEs. Their abundances could not be measured, but those of the HREEs can be estimated from the Y abundance, which is ~0.1 × CI (Fig. 3). A few of the other elements (Sc, Sr, Ba, V, Cr, Li, K, and B) have abundances around 1 × CI. However, two elements have abundances that are very high: Zr (760 × CI) and Be (520). The co-existing glass is also rich in these elements, but their abundances are not high enough for a chemical equilibrium between rutile and a former glassy matrix. Very few partition coefficients for rutile/silicate liquid are known (Jenner et al. 1993) for Sr = 0.5 and for Zr = 5. Given these (highest values found), the rutile appears to be totally out of equilibrium with the glass with a rutile-glass distribution ratio of 97 for Zr, but it could have crystallized from a liquid containing 152 × CI Zr. These data and the high Be content suggest an exotic source for the rutile. Because rutile is not known to be a phase that can directly precipitate from the solar nebula, it very likely had a precursor, presumably one from the clan of Ti-rich phases usually associated with oldhamite in E meteorites. The low REE abundances in rutile point toward osbornite as a possible precursor (e.g., Kurat et al. 1992), which was oxidized to rutile. The source for the high Be content is unknown and currently subject of an investigation—as is the Zr problem.

Magnetite

Magnetite is not part of the silicate inclusion assemblage in Guin, but rather enclosed separately in the metal. Its occurrence and co-existence with rust suggests a secondary origin from a former assemblage that contained lawrencite. Trace element contents are all very low, indicating a lithophile-element–poor, metal-related source. However, many hydrophile elements are present at detectable abundance levels, which indicate that possibly terrestrial water was involved in the oxidation event.

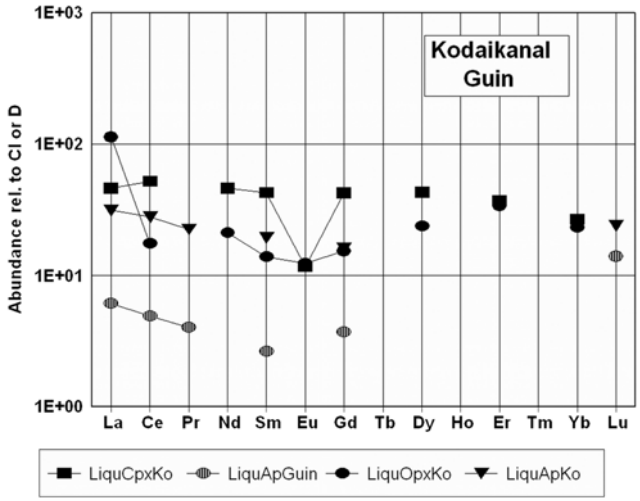

Fig. 13. CI-normalized estimated liquid REE contents in equilibrium with pyroxenes and apatites in the Guin (UNGR) and Kodaikanal IIE iron meteorites. Liquid in equilibrium with pyroxenes and apatite in the Kodaikanal inclusion have similar compositions and indicate crystallization from a trace element–rich liquid with about 10–50 × CI abundances (the universal liquid of Varela and Kurat 2004 and Kurat et al. 2004). Apatite from Guin apparently has a source different from that in Kodaikanal. However, both of them are far out of chemical equilibrium with the glass they are now associated with.

Hypothetical Liquid Compositions

Estimates for abundances of REEs in the liquids that could have crystallized the pyroxenes and apatite in Kodaikanal range between 12 and 55 × CI, all with flat patterns but at different levels: clinopyroxene needs a liquid with REEs near 50 × CI and low Ca-pyroxene and apatite a liquid with REE ~20 × CI (Fig. 13). Hence, two different liquids are indicated for the production of silicates and apatite in Kodaikanal inclusion 2, both in the range of bulk CAI compositions. However, given all the uncertainties these data contain, they could be taken as to indicate a single, refractory-element–rich liquid. Ruzicka et al. (1999, 2006) and Hsu (2003) reported very similar hypothetical liquid compositions for the Mg/Fe phases in the Weekeroo Station IIE, Sombrerete (UNGR) and Miles IIE irons, except for a few that look fractionated but shall not concern us here. Such liquids are predicted to be present in the solar nebula under higher-than-canonical pressure regimes (e.g., Yoneda and Grossman 1995), appear to be omnipresent in the early solar nebula and to be responsible for the formation of almost all rocks we get delivered as meteorites (e.g., Varela and Kurat 2004, 2006). Therefore, it is possible that the Kodaikanal silicates also formed from and with the help of such liquids. If this is indeed the case, then the proto-inclusions for Kodaikanal formed from liquids that directly condensed from the solar nebula vapor at high T and p conditions.

A New Model for IIE Silicate Inclusion Formation

Recent attempts to model the formation of these rocks by conventional magmatic approaches have met insurmountable difficulties and reached nonsatisfying conclusions such as "IIE iron meteorites could have formed by the collision between an FeNi metal impactor and either a differentiated or undifferentiated silicate-rich target of H-chondrite affinity. More than one type of target may be necessary to account for the full diversity of IIE-like meteorites." (Ruzicka et al. 1999). Takeda et al. (2003) concluded that "these assemblages cannot be made by impact melting of the H chondrites"—a widely entertained model. Because none of the proposed models can explain the existing wealth of contradictory data, the obvious nonequilibria between co-existing phases, the strange elemental fractionations with some incompatible elements being depleted, others enriched, the high abundance of apatite (about 10 vol% in near-surface glass) (Fig. 6), the common presence of Eu and Yb abundance anomalies, the complementary abundance anomalies in apatite and glass and many other features, we offer here an incomplete alternative model for future tests and discussion.

If we consider the Kodaikanal inclusions, they could have formed from a nebular refractory liquid that precipitated in the first stage diopside, which at that stage acquired its refractory trace element abundance. The lack of olivine in the assemblage points to the refractory nature of the clinopyroxene-liquid assembly, the early condensing CAI-related CMAS liquid of Yoneda and Grossman (1995). An alternative possibility would be a strongly fractionated nebula composition, which had to be depleted in condensable Mg as compared to the standard solar nebula composition. Anyway, possible ways to achieve that goal shall be investigated in the future especially because similar liquids are also needed for the formation of pyroxene-rich achondritic rocks (e.g., angrites, nakhlites, eucrites). The Kodaikanal primary silicate liquid obviously precipitated first diopside (low-Al augite). Addition of P to the system—by condensation from the vapor or by dissolution of P-bearing phases—created a demand for Ca for the formation of phosphates, which as a consequence led to dissolution of the previously precipitated augite and its partial replacement by low-Ca pyroxene. At that point the liquid was still rich in refractory trace elements (as documented by the precipitated phases) but was already poor in Ca, which was utilized for the formation of phosphates and was probably replaced by alkalis from the vapor. The alkalis must have been fractionated from each other either by gaseous or crystalline species akin to sulfides such as djerfisherite ($K_6[Cu,Fe,Ni]_{25}S_{26}Cl$) and caswellsilverite ($NaCrS_2$) from which the alkalis were liberated by oxidation and entered the silicate liquid in stochastic, nonchondritic proportions. After quenching of the liquid, the crystal phases, augite, enstatite, and apatite, were left embedded in a glass that was rich in refractory elements and possibly also alkalis. In addition to the metasomatic processes that were already at work up to this stage (addition of P and vapor-liquid exchange of alkalis for Ca), several metasomatic events must have taken place likely in the subsolidus temperature range:

- exchange of Mg from the silicates for Fe, "equilibration" of the pyroxene composition (see, e.g., Kurat 1988) under conditions similar to those prevailing in the OC chondrite formation region;
- equilibration of the O isotopes of the rock with those of the vapor—also in the OC chondrite formation region (H chondrite for IIE inclusions [Clayton et al. 1983], LL chondrite for Guin [Rubin et al. 1985]);
- exchange of Mg for moderately volatile elements, such as Cr and Mn—also in the OC chondrite formation region;
- removal of elements that could be mobilized (up to +3-charged ions, including the REEs, but not HFSEs) from the glass (where diffusion is fast) but not from the crystalline phases (where diffusion is slow) to the vapor (see, e.g., Engler et al. 2004).

The model for the formation of the Guin (UNGR) silicate inclusion investigated is similar to that given above for Kodaikanal. The record left in the inclusion allows us to reconstruct the following possible genetic pathway:

- in a strongly reducing nebular vapor, CaS (and possibly also TiN) was precipitated at high *T*, took all refractory lithophile elements available, in particular the refractory REEs (Lodders and Fegley 1993), and left behind a vapor, which was depleted in these elements;
- from that fractionated vapor a silica-rich liquid, poor in REEs but rich in Eu and Yb and CaS-incompatible refractory elements (e.g., Al, Ti, Nb), precipitated and was chilled;
- the products CaS—and possibly also TiN—were transferred into an oxidizing nebular region (similar to the LL chondrite formation region), where the reduced phases were oxidized and transformed into apatite and rutile, respectively;
- here also, O was exchanged with the vapor and adjusted to an isotopic composition similar to that of LL chondrites;
- Ca from the glass was exchanged for alkalis from an unfractionated chondritic vapor.

Inclusions in IIE irons range in composition from chondritic to highly fractionated, alkali-, pyroxene- and even silica-rich. The suggested nebular processes can produce the whole spectrum of inclusion rocks simply by changing the Mg/Si ratio in the vapor. Changes in that ratio can best be achieved by locking Mg into a silica-free phase, like niningerite, or comparable gas species. A vapor with chondritic Mg/Si ratio should produce olivine-bearing proto-rocks such as olivine-anorthite, olivine-clinopyroxene rocks, and Mg-depleted vapor protorocks like E meteorites. High temperatures in the solar nebula in regions with redox

conditions similar to those experienced by OCs led to oxidation of previously formed sulfides (oldhamite, niningerite, alkali-sulfides) and other phases (e.g., osbornite), to a Mg-Fe, Ca-alkali, and O exchange between vapor and the silicate phases, and to homogeneous, equilibrated OC-like mineral compositions.

The final product could be glass-rich objects such as those we observe now as inclusions in FeNi metal. These objects appear to have been overgrown first by schreibersite and then gently been enclosed by metal produced in a subsolidus process from carbonyls as suggested by Bloch and Müller (1971) and discussed by Kurat (2003).

CONCLUSIONS

Phases in glass-bearing multiphase silicate inclusions in the genetically related Guin (UNGR) and Kodaikanal (IIE) irons are chemically far out of equilibrium and strongly fractionated, as previously observed in several IIE irons. From the discussion above, it is evident that the solution of most problems posed by the Guin and Kodaikanal inclusions (and all other IIE iron silicate inclusions) lies in the solar nebula. Our data suggest that nebular condensation and subsolidus nebular processing were responsible for the formation of these rocks—as they appear to be for most meteoritic matter. What becomes immediately evident is that the story starts in a highly reducing environment with condensation of refractory minerals and liquids (CAI-related) and ends with elemental exchange reactions between solids and the cooling vapor under oxidizing condition—a sequence of events recorded in most meteorites. The case of the IIE iron and Guin silicate inclusions appears to be no special case, except for the size of the objects (cm-sized instead of mm-sized like chondritic constituents) and their location (in metal instead of a silicate rock, chondritic or achondritic).

The few phases present in Guin do not provide us with a comprehensive genetic story but give us clear evidence for high *T* condensation under reducing conditions and metasomatism under oxidizing conditions. The condensation event is recorded by the presence of large apatite and rutile, which likely are derivatives of reduced early condensates such as oldhamite and osbornite. The devitrified glass associated with these phases has complementary REE abundances to those of the apatite, clearly indicating a condensation relationship, with the apatite being depleted and the glass being enriched in the moderately volatile REEs Eu and Yb relative to the neighboring REEs. High contents of alkalis (in fractionated as well as unfractionated proportions) and other volatile elements in the glass document a metasomatic exchange with the cooling nebula, a process previously identified for chondritic constituents like chondrules.

Silicate inclusions in Kodaikanal contain a record of high *T* condensation from a non-fractionated nebular reservoir. The vapor produced a liquid that was rich in refractory trace elements and precipitated mainly clinopyroxene, some low-Ca pyroxene, and apatite. These three phases kept a memory of their derivation from a refractory element-rich liquid. This liquid was quenched and is now present as glass. However, the chemical composition of this glass is not refractory any more, but has been changed to be siliceous, alkali-rich, and REE-poor. This composition appears to be the result of a metasomatic exchange between the glass and the cooling nebula. In that process the REEs were removed (and probably stored in a phase outside the glass—see e.g., Engler et al. 2004) and alkalis and other volatile elements were added to the glass. That process seems to have taken place in an environment similar to that in which the constituents of the OCs were processed: the Fe/Mg ratio of the silicates and O isotopic ratios were changed to those of OCs.

Finally, the rocks created in this way were gently covered by condensing schreibersite and wrapped up into metal (via low-temperature condensation, possibly from carbonyl breakdown), where we can find them now unscratched for our investigations.

Inclusions found in other IIE irons can be created in the same way but had to start out at different condensation *p-T* conditions: the whole range is represented, from unfractionated (chondritic inclusions, e.g., Netschaevo) to highly fractionated rocks and glasses, e.g., in Kodaikanal. The latter seem to have been derived from phases and liquids (CAIs) condensing at high temperature under generally reducing conditions. These phases were subsequently oxidized and metasomatically altered to alkali- and Si-rich rocks.

Acknowledgments–We thank Andrey Gurenko and Nora Groschopf, Mainz, for the use of and for help with the EMP in Mainz, Theodoros Ntaflos and Franz Brandstätter for support with the EMPAs in Vienna, Svetlana Demidova for help with the ASEM, and Christine Floss for help with the ion microprobe. Reviews by John Wasson, Alex Ruzicka, and associate editor Kevin Righter helped to considerably improve the report. Financial support was received in Austria from FWF (P16420-N10), in Argentina from CONICET (FWF-CONICET and PIP 5005), and in the USA from NASA grant NNG04GG49G (Christine Floss, PI).

Editorial Handling—Dr. Kevin Righter

REFERENCES

Alexander C. M. O'D. 1994. Trace element distributions within ordinary chondrite chondrules: Implications for chondrule formation conditions and precursors. *Geochimica et Cosmochimica Acta* 58:3451–3467.

Alexander E. C., Jr. and Manuel O. K. 1968. Xenon in the inclusions of Canyon Diablo and Toluca iron meteorites. *Earth and Planetary Science Letters* 4:113–117.

Anders E. and Grevesse N. 1989. Abundances of the elements: Meteoritic and solar. *Geochimica et Cosmochimica Acta* 53:197–214.

Asame K., Kawano S., Matsuda J. I., Maruoka T., and Kurat G. 1999. Nitrogen isotopic signatures of metal and graphite in Canyon Diablo (abstract). 24th Symposium on Antarctic Meteorites. pp. 1–3.

Bence A. E. and Burnett D. S. 1969. Chemistry and mineralogy of the silicates and metal of the Kodaikanal meteorite. *Geochimica et Cosmochimica Acta* 33:387–407.

Birck J. L. and Allegre C. J. 1998. Rhenium-187–osmium-187 in iron meteorites and the strange origin of the Kodaikanal meteorite. *Meteoritics & Planetary Science* 33:647–653.

Bloch M. R. and Müller O. 1971. An alternative model for the formation of iron meteorites. *Earth and Planetary Science Letters* 12:134–136.

Bogard D. D., Burnett D., Eberhardt P., and Wasserburg G. J. 1967. ^{40}Ar-^{40}K ages of silicate inclusions in iron meteorites. *Earth and Planetary Science Letters* 3:275–283.

Bogard D. D., Burnett D., Eberhardt P., and Wasserburg G. J. 1969. Cosmogenic rare gases and the ^{40}Ar-^{40}K age of the Kodaikanal iron meteorite. *Earth and Planetary Science Letters* 5:273–281.

Bogard D. D., Huneke J. C., Burnett D. S., and Wasserburg G. J. 1971. Xe and Kr analyses of silicate inclusions from iron meteorites. *Geochimica et Cosmochimica Acta* 35:1231–1254.

Bogard D. D., Garrison D. H., and McCoy T. J. 2000. Chronology and petrology of silicates from IIE meteorites: Evidence of a complex parent body evolution. *Geochimica et Cosmochimica Acta* 64: 2133–2154.

Brearley A. J. and Jones R. H. 1998. Chondritic meteorites. In *Planetary materials*, edited by Papike J. J. Reviews in Mineralogy, vol. 36. Washington, D. C.: Mineralogical Society of America. pp. 3-1–3-394.

Buchwald V. F. 1975. *Handbook of iron meteorites: Their history, distribution, composition and structure*. Berkeley: University of California Press. 1418 p.

Bunch T. E., Keil K., and Olsen E. 1970. Mineralogy and petrology of silicate inclusions in iron meteorites. *Contributions to Mineralogy and Petrology* 25:297–340.

Burnett D. S. and Wasserburg G. J. 1967. ^{87}Rb-^{87}Sr ages of silicate inclusions in iron meteorites. *Earth and Planetary Science Letters* 2:397–408.

Casanova I., Graf T., and Marti K. 1995. Discovery of an unmelted H-chondrite inclusion in an iron meteorite. *Science* 268:540–542.

Chen J. H. and Wasserburg G. J. 1983. The isotopic composition of silver and lead in two iron meteorites: Cape York and Grant. *Geochimica et Cosmochimica Acta* 47:1725–1737.

Clarke R. S., Jr. and Goldstein J. I. 1978. *Schreibersite growth and its influence on the metallography of coarse structured iron meteorites*. Smithsonian Contributions to Earth Sciences 21. 80 p.

Clayton R. N., Mayeda T. K., Olsen E. J., and Prinz M. 1983. Oxygen isotope relationships in iron meteorites. *Earth and Planetary Science Letters* 65:229–232.

Crozaz G. and Lundberg L. L. 1995. The origin of oldhamite in unequilibrated enstatite chondrites. *Geochimica et Cosmochimica Acta* 59:3817–3831.

Deines P. and Wickman F. E. 1975. A contribution to the stable carbon isotope geochemistry of iron meteorites. *Geochimica et Cosmochimica Acta* 39:547–557.

Dohmen R. and Chakraborty S. 2003. Mechanism and kinetics of element and isotopic exchange mediated by a fluid phase. *American Mineralogist* 88:1251–1270.

Dohmen R., Chakraborty S., Palme H., and Rammensee W. 1998. Solid-solid reactions mediated by a gas phase: An experimental study of reaction progress and the role of surfaces in the system olivine + Fe-metal. *American Mineralogist* 83:970–984.

Ebihara M., Ikeda Y., and Prinz M. 1997. Petrology and chemistry of the Miles IIE iron. II—Chemical characteristics of the Miles silicate inclusions. *Antarctic Meteorite Research* 10: 373–388.

El Goresy A. 1965. Mineralbestand und Strukturen der Graphit- und Sulfideinschlüsse in Eisenmeteoriten. *Geochimica et Cosmochimica Acta* 29:1131–1151.

El Goresy A., Yabuki H., Ehlers K., Woolum D., and Pernicka E. 1988. Qingzhen and Yamato-691: A tentative alphabet for the EH chondrites. *Proceedings of the NIPR Symposium on Antarctic Meteorites* 1:65–101.

Engler A., Kurat G., and Sylvester P. J. 2004. Trace element abundances in chondrules from Knyahinya (L/LL5) and Ouzina (R4) (abstract). *Meteoritics & Planetary Science* 39:A37.

Fahey A. J., Zinner E., Kurat G., and Kracher A. 1994. Hibonite-hercynite inclusion HH-1 from the Lance (CO3) meteorite: The history of an ultrarefractory CAI. *Geochimica et Cosmochimica Acta* 58:4779–4793.

Fegley B., Jr. 2000. Kinetics of gas-grain reactions in the solar nebula. *Space Science Reviews* 91:107–130.

Franchi I. A., Wright I. P., and Pillinger C. T. 1993. Constraints on the formation conditions of iron meteorites based on concentrations and isotopic compositions of nitrogen. *Geochimica et Cosmochimica Acta* 57:3105–3121.

Green T. H. 1994. Experimental studies of trace-element partitioning applicable to igneous petrogenesis—Sedona 16 years later. *Chemical Geology* 117:1–36.

Haack H. and Scott E. R. D. 1992. Asteroid core crystallization by inward dendritic growth. *Journal of Geophysical Research* 97: 727–743.

Haack H., Scott E. R. D., Love S. G., Brearley A. J., and McCoy T. J. 1996. Thermal histories of IVA stony-iron and iron meteorites: Evidence for asteroid fragmentation and reaccretion. *Geochimica et Cosmochimica Acta* 60:3103–3113.

Harper C. L. and Jacobsen S. B. 1996. Evidence for ^{182}Hf in the early solar system and constraints on the time scale of terrestrial accretion and core formation. *Geochimica et Cosmochimica Acta* 60:1131–1153.

Hoinkes G. and Kurat G. 1974. Chemismus von Spinellen aus dem Mezö-Madaras-Chondrit. In *Analyse extraterrestrischen Materials*, edited by Kiesl W. and Malissa H., Jr. Vienna: Springer-Verlag. pp. 265–288.

Hsu W. 1995. Ion microprobe studies of the petrogenesis of enstatite chondrites and eucrites. Ph.D. thesis. Washington University, Saint Louis, Missouri, USA.

Hsu W. 2003. Rare earth element geochemistry and petrogenesis of Miles (IIE) silicate inclusions. *Geochimica et Cosmochimica Acta* 67:4807–4821.

Ireland T. R., Fahey A. J., and Zinner E. K. 1988. Trace-element abundances in hibonites from the Murchison carbonaceous chondrite: Constraints on high-temperature processes in the solar nebula. *Geochimica et Cosmochimica Acta* 52:2841–2854.

Jenner G. A., Foley S. F., Jackson S. E., Green T. H., Fryer B. J., and Longerich H. P. 1993. Determination of partition coefficients for trace elements in high pressure-temperature experimental run products by laser ablation microprobe-inductively coupled plasma mass spectrometry (LAM-ICP-MS). *Geochimica et Cosmochimica Acta* 57:5099–5103.

Jochum K. P., Seufert M., and Begemann F. 1980. On the distribution of major and trace elements between metal and phosphide phases of some iron meteorites. *Zeitschrift für Naturforschung* 35b:57–63.

Jones J. H. and Malvin D. J. 1990. A nonmetal interaction model for

the segregation of trace metals during solidification of Fe-Ni-S, Fe-Ni-P, and Fe-Ni-S-P alloys. *Metallurgical and Materials Transactions B* 21:697–706.

Kaiser T. and Wasserburg G. J. 1983. The isotopic composition and concentration of Ag in iron meteorites and the origin of exotic silver. *Geochimica et Cosmochimica Acta* 47:43–58.

Keil K. and Fredriksson K. 1964. The iron, magnesium, and calcium distribution in coexisting olivines and rhombic pyroxenes in chondrites. *Journal of Geophysical Research* 64:3487–3515.

Keil K., Ntaflos T., Taylor G. J., Brearley A. J., Newsom H. E., and Romig A. D., Jr. 1989. The Shallowater aubrite: Evidence for origin by planetesimal impact. *Geochimica et Cosmochimica Acta* 53:3291–3307.

Kleine T., Mezger K., Palme H., Scherer E., and Münker C. 2005. Early core formation in asteroids and late accretion of chondrite parent bodies: Evidence from ^{182}Hf-^{182}W in CAIs, metal-rich chondrites, and iron meteorites. *Geochimica et Cosmochimica Acta* 69:5805–5818.

Kracher A. 1974. Untersuchungen am Landes Meteoriten. In *Analyse extraterrestrischen Materials*, edited by Kiesl W. and Malissa H. Vienna: Springer-Verlag. pp. 315–326.

Kurat G. 1967. Einige Chondren aus dem Meteoriten von Mezö-Madaras. *Geochimica et Cosmochimica Acta* 31:1843–1857.

Kurat G. 1988. Primitive meteorites: An attempt towards unification. *Philosophical Transactions of the Royal Society London A* 325: 459–482.

Kurat G. 2003. Why iron meteorites cannot be samples of planetesimal smelting (abstract). Evolution of Solar System Materials: A New Perspective from Antarctic Meteorites. pp. 65–66.

Kurat G. and Kracher A. 1980. Basalts in the Lancé carbonaceous chondrite. *Zeitschrift für Naturforschung* 35a:180–190.

Kurat G., Pernicka E., and Herrwerth I. 1984. Chondrules from Chainpur (LL-3): Reduced parent rocks and vapor fractionation. *Earth and Planetary Science Letters* 68:43–56.

Kurat G., Brandstaetter F., Palme H., and Spettel B. 1991. Non-equilibria in the Acuña IIIAB iron. 22nd Lunar and Planetary Science Conference. pp. 767–768.

Kurat G., Zinner E., and Brandstätter F. 1992. An ion microprobe study of an unique oldhamite-pyroxenite fragment from the Bustee aubrite (abstract). *Meteoritics* 26:246.

Kurat G., Nazarov M. A., Brandstätter F., Ntaflos T., and Koeberl C. 1997. Precipitation and reaction products of fluids in Martian orthopyroxenite ALH 84001 (abstract). 28th Lunar and Planetary Science Conference. pp. 777–778.

Kurat G., Sylvester P., Kong P., and Brandstätter F. 2000. Heterogeneous and fractionated metal in Canyon Diablo (IA) graphite—Metal rock (abstract #1666). 31st Lunar and Planetary Science Conference. CD-ROM.

Kurat G., Varela M. E., Ametrano S. J., and Brandstätter F. 2002a. Major, minor, and trace element abundances in metal and schreibersite of the San Juan mass of Campo del Cielo (IAB) (abstract #1781). 33rd Lunar and Planetary Science Conference. CD-ROM.

Kurat G., Zinner E., and Brandstätter F. 2002b. A plagioclase-olivine-spinel-magnetite inclusion from Maralinga (CK): Evidence for sequential condensation and solid-gas exchange. *Geochimica et Cosmochimica Acta* 66:2959–2979.

Kurat G., Varela M. E., Zinner E., and Engler A. 2004. Condensation origin model for chondrules (abstract). *Meteoritics & Planetary Science* 39:A57.

Kurat G., Varela M. E., and Zinner E. 2005. Silicate inclusions in the Kodaikanal IIE iron meteorite (abstract #1814). 36th Lunar and Planetary Science Conference. CD-ROM.

Kurat G., Zinner E., Varela M. E., and Demidova S. I. 2006. A nebular origin of chlorapatite and silicate glass in the Guin (UNGR) iron (abstract). *Meteoritics & Planetary Science* 41:A102.

Litvin Y. A. and Zharikov V. A. 1999. Primary fluid-carbonatite inclusions in diamond: Experimental modeling in the system K_2O-Na_2O-CaO-MgO-FeO-CO_2 as a diamond formation medium at 7–9 GPa. *Doklady Earth Sciences* 367A:801–805.

Lodders K. 2003. Solar system abundances and condensation temperatures of the elements. *The Astrophysical Journal* 591: 1220–1247.

Lodders K. and Fegley B., Jr. 1993. Lanthanide and actinide chemistry at high C/O ratios in the solar nebula. *Earth and Planetary Science Letters* 117:125–145.

Martin P. M. and Mason B. 1974. Major and trace elements in the Allende meteorite. *Nature* 249:333–334.

Maruoka T., Kurat G., Zinner E., Varela M. E., and Ametrano S. J. 2003. Carbon isotopic heterogeneity of graphite in the San Juan mass of the Campo del Cielo IAB iron meteorite (abstract #1663). 34th Lunar and Planetary Science Conference. CD-ROM.

Matsuda J. I., Namba M., Maruoka T., Matsumoto T., and Kurat G. 2005. Primordial noble gases in a graphite-metal inclusion from the Canyon Diablo IAB iron meteorite and their implications. *Meteoritics & Planetary Science* 40:431–443.

McKay G., Wagstaff J., and Yang S. R. 1986. Clinopyroxene REE distribution coefficients for shergottites: The REE content of the Shergotty melt. *Geochimica et Cosmochimica Acta* 50:927–937.

Meshik A., Kurat G., Pravdivtseva O., and Hohenberg C. M. 2004. Radiogenic 129-xenon in silicate inclusions in the Campo del Cielo iron meteorite (abstract #1687). 35th Lunar and Planetary Science Conference. CD-ROM.

Mittlefehldt D. W., McCoy T. J., Goodrich C. A., and Kracher A. 1998. Non-chondritic meteorites from asteroidal bodies. In *Planetary materials*, edited by Papike J. J. Reviews in Mineralogy, vol. 36. Washington, D. C.: Mineralogical Society of America. pp. 1–195.

Navon O., Hutcheon I. D., Rossman G. R., and Wasserburg G. J. 1988. Mantle-derived fluids in diamond micro-inclusions. *Nature* 335: 784–789.

Nehru C. E., Prinz M., and Delaney J. S. 1982. The Tucson iron and its relationship to enstatite meteorites. Proceedings, 13th Lunar and Planetary Science Conference. pp. A365–A373.

Niemeyer S. 1979. I-Xe dating of silicate and troilite from IAB iron meteorites. *Geochimica et Cosmochimica Acta* 43:843–860.

Peck J. A. and Wood J. A. 1987. The origin of ferrous zoning in Allende chondrule olivines. *Geochimica et Cosmochimica Acta* 51:1503–1510.

Prinz M., Nehru C. E., Delaney J. S., Weisberg M., and Olsen E. 1983. Globular silicate inclusions in IIE irons and Sombrerete: Highly fractionated minimum melts (abstract). 14th Lunar and Planetary Science Conference. pp. 618–619.

Prowatke S. and Klemme S. 2006. Trace element partitioning between apatite and silicate melts. *Geochimica et Cosmochimica Acta* 70:4513–4527.

Quitte G., Birck J. L., and Allegre C. J. 2000. ^{182}Hf-^{182}W systematics in eucrites: The puzzle of iron segregation in the early solar system. *Earth and Planetary Science Letters* 184:83–94.

Quitte G., Meier M., Latcoczy C., Halliday A. N., and Günther D. 2006. Nickel isotopes in iron meteorites-nucleosynthetic anomalies in sulfides with no effects in metals and no trace of ^{60}Fe. *Earth and Planetary Science Letters* 242:16–25.

Rambaldi E. R., Fredriksson B. J., and Fredriksson K. 1981. Primitive ultrafine matrix in ordinary chondrites. *Earth and Planetary Science Letters* 56:107–126.

Rasmussen K. L., Ulff-Møller F., and Haack H. 1995. The thermal evolution of IVA iron meteorites: Evidence from metallographic

cooling rates. *Geochimica et Cosmochimica Acta* 59:3049–3059.

Rubin A. E., Jerde E. A., Zong P., Wasson J. T., Westcott J. W., Mayeda T. K., and Clayton R. N. 1986. Properties of the Guin ungrouped iron meteorite: The origin of Guin and of group-IIE irons. *Earth and Planetary Science Letters* 76:209–226.

Ruzicka A., Fowler G. W., Snyder G. A., Prinz M., Papike J. J., and Taylor L. A. 1999. Petrogenesis of silicate inclusions in the Weekeroo Station IIE iron meteorite: Differentiation, remelting, and dynamic mixing. *Geochimica et Cosmochimica Acta* 63: 2123–2143.

Ruzicka A., Hutson M., and Floss C. 2006. Petrology of silicate inclusions in the Sombrerete ungrouped iron meteorite: Implications for the origin of IIE-type silicate-bearing irons. *Meteoritics & Planetary Science* 41:1797–1831.

Sanz H. G., Burnett D. S., and Wasserburg G. J. 1970. A precise $^{87}Rb/^{87}Sr$ age and initial $^{87}Sr/^{86}Sr$ for the Colomera iron meteorite. *Geochimica et Cosmochimica Acta* 34:1227–1239.

Schersten A., Elliott T., Hawkesworth C., Russell S., and Mazarik J. 2006. Hf-W evidence for rapid differentiation of iron meteorite parent bodies. *Earth and Planetary Science Letters* 241:530–542.

Schwandt C. S. and McKay G. A. 1996. REE partition coefficients from synthetic diogenite-like enstatite and the implications of petrogenetic modeling (abstract). Workshop on Evolution of Igneous Asteroids: Focus on Vesta and the HED meteorites. p. 25.

Scott E. R. D. 1979. Origin of iron meteorites. In *Asteroids*, edited by Gehrels T. Tucson, Arizona: The University of Arizona Press. pp. 892–921.

Skala R., Fryda J., and Sekanina J. 2000. Mineralogy of the Vicenice octahedrite. *Journal of the Czech Geological Society* 45:175–192.

Snyder G. A., Lee D. C., Ruzicka A. M., Prinz M., Taylor L. A., and Halliday A. N. 2001. Hf-W, Sm-Nd, and Rb-Sr isotopic evidence of late impact fractionation and mixing of silicates on iron meteorite parent bodies. *Earth and Planetary Science Letters* 186:311–324.

Sokol A. G., Tomilenko A. A., Pal'yanov Y. N., Borzdov Y. M., Pal'yanova G. A., and Khokhryakov A. F. 2000. Fluid regime of diamond crystallisation in carbonate-carbon system. *European Journal of Mineralogy* 12:367–375.

Strange P., Svane A., Temmermann W. M., Szotek Z., and Winters H. 1999. Understanding the valency of rare earths from first-principles theory. *Nature* 399:756–758.

Sugiura N. 1998. Ion probe measurements of carbon and nitrogen in iron meteorites. *Meteoritics & Planetary Science* 33:393–409.

Sugiura N. and Hoshino H. 2003. Mn-Cr chronology of five IIIAB iron meteorites. *Meteoritics & Planetary Science* 38:117–143.

Takeda M. H., Hsu W., and Huss G. 2003. Mineralogy of silicate inclusions of the Colomera IIE iron and crystallization of Cr-diopside and alkali feldspar from a partial melt. *Geochimica et Cosmochimica Acta* 67:2269–2288.

Taylor S. R. 1992. *Solar system evolution: A new perspective*. Cambridge: Cambridge University Press. 307 p.

Tuttle O. F. and Bowen N. L. 1958. Origin of granite in the light of experimental studies in the system $NaAlSi_3O_8$-$KalSi_3O_8$-SiO_2-H_2O. New York: The Geological Society of America. 153 p.

Varela M. E. and Kurat G. 2004. Glasses in meteorites: A unification model (abstract). *Meteoritics & Planetary Science* 39:A109.

Varela M. E. and Kurat G. 2006. A universal meteorite formation process (abstract). *Meteoritics & Planetary Science* 41:A180.

Varela M. E., Kurat G., Clocchiatti R., and Schiano P. 1998. The ubiquitous presence of silica-rich glass inclusions in mafic minerals: Examples from Earth, Mars, Moon and the aubrite parent body. *Meteoritics & Planetary Science* 33:1041–1051.

Varela M. E., Kurat G., Bonnin-Mosbah M., Clocchiatti R., and Massare D. 2000. Glass-bearing inclusions in olivine of the Chassigny achondrite: Heterogeneous trapping at subigneous temperatures. *Meteoritics & Planetary Science* 35:39–52.

Varela M. E., Kurat G., Zinner E., Métrich N., Brandstätter F., Ntaflos T., and Sylvester P. 2003. Glasses in the D'Orbigny angrite. *Geochimica et Cosmochimica Acta* 67:5027–5046.

Varela M. E., Kurat G., and Zinner E. 2005. A liquid-supported condensation of major minerals in the solar nebula: Evidence from glasses in the Kaba (CV3) chondrite. *Icarus* 178:553–569.

Varela M. E., Kurat G., and Zinner E. 2006. The primary liquid condensation model and the origin of barred olivine chondrules. *Icarus* 184:344–364.

Wasson J. T. 1968. Concentrations of nickel, gallium, germanium, and iridium in Canyon Diablo and other Arizona octahedrites. *Journal of Geophysical Research* 73:3207–3211.

Wasson J. T. 1985. *Meteorites: Their record of early solar system history.* New York: Freeman. 267 p.

Wasson J. T. and Wang J. 1986. A nonmagmatic origin of group-IIE iron meteorites. *Geochimica et Cosmochimica Acta* 50:725–732.

Wlotzka F. 2005. Cr spinel and chromite as petrogenetic indicators in ordinary chondrites: Equilibrium temperatures of petrologic types 3.7 to 6. *Meteoritics & Planetary Science* 40:1673–1702.

Wlotzka F., Palme H., Spettel B., Wänke H., Fredriksson K., and Noonan A. F. 1983. Alkali differentiation in LL chondrites. *Geochimica et Cosmochimica Acta* 47:743–757.

Yoneda S. and Grossman L. 1995. Condensation of CaO-MgO-Al_2O_3-SiO_2 liquids from cosmic gases. *Geochimica et Cosmochimica Acta* 59:3413–3444.

Zinner E. and Crozaz G. 1986a. A method for the quantitative measurement of rare earth elements in the ion microprobe. *International Journal of Mass Spectrometry and Ion Processes* 69:17–38.

Zinner E. and Crozaz G. 1986b. Ion probe determination of the abundances of all the rare earth elements in single mineral grains. In *Secondary ion mass spectrometry,* edited by Benninghoven A., Colton J., Simons D. S., and Werner H. W. New York: Springer-Verlag. pp. 444–446.